



Dynamic simulation of urban growth and land use change using an integrated cellular automata and markov chain models: a case of Bahir Dar city, Ethiopia

Kenu Getu^{1,2} · H. Gangadhara Bhat¹

Received: 4 September 2021 / Accepted: 10 May 2022 / Published online: 24 May 2022
© Saudi Society for Geosciences 2022

Abstract

In recent decades, the rapid growth of cities has been a recognizable hallmark of urban expansion, particularly in third world/economically developing nations like Ethiopia. To address this problem, it is necessary to project/simulate the spread of urban areas over time to avoid unplanned and illegal growth of urban areas to natural and agricultural land. Though GIS, RS, and CA–Markov models have been used to investigate urban expansion in different countries, including Ethiopia, no critical study has been applied to examine urban growth and LULC change in Bahir Dar. From 1984 to 2019, there was a significant change in land use in this area. Significant changes occurred from 1984 to 2019 in crop land (11.3%), followed by built-up (10.76%) and wetland (3.36%). The future growth of Bahir Dar is predicted for the years 2029, 2039, and 2049. The result indicated a high rate of urban growth with an expansion predicted to develop of 28.83, 31.14, and 34.98 m² for the coming years of 2029, 2039, and 2049, respectively in Bahir Dar and its surroundings. The kappa index values of K_{no} and $K_{location}$ were found to be 0.0.8816 and 0.8799, respectively, which indicates a strong agreement between the actual and predicted thematic maps for the year 2019. The results also revealed that the city's development in the eastern and western fronts will be more intense and faster in the upcoming years compared to the other regions. To summarize, this model is an effective and efficient tool that supports urban design and planning decisions and facilitates sustainable urban development processes.

Keywords Urban growth · Cellular automata · Markov chain · Transition potential · Bahir Dar

Abbreviations

AHP	Analytical hierarchy processes
CA	Cellular automata
CBD	Central business district
CR	Consistency ratio
DEM	Digital elevation model
GDP	Gross domestic product
GIS	Geographic information system
LU	Land use
LULC	Land use land cover change

MC	Markov chain model
MCE	Multi-criteria evaluations
RI	Random index
RS	Remote sensing

Introduction

Urbanization is the most contemporary phenomenon of urban development, which is also called urban revolution (Turok and McGranahan 2013). According to UN predictions, the urban areas will inhabit more than half (50%) of the rural population by 2050. This phenomenon is one of the major problems in most regions of the world, as chaotic urbanization and lack of good planning have resulted in the expansion of unplanned urban areas (Jafari et al. 2016). Rapid urban expansion, in developing nations in particular, is accompanied by major socio-economic problems (Nguyen 2015). This phenomenon is accomplished by misusing natural resources, which directly disturbs the urban ecosystem and makes the urban environment more susceptible to many

Responsible Editor: Biswajeet Pradhan

✉ Kenu Getu
kenugetu@gmail.com

H. Gangadhara Bhat
gangadharrbhat@gmail.com

¹ Department of Marine Geology, Mangalore University, Mangalagangothri, Karnataka, India

² Department of Geography and Environmental Studies, Debre Tabor University, P.O. Box 272, Debre Tabor, Ethiopia

enforced risks (Keith et al. 2019; Kharel 2010; Cui et al. 2019).

The rapid urban growth and land use land cover (LULC) transformation led researchers and decision-makers to give much attention to the impacts of rapid urban growth on the ecosystem and livelihood of the people (Hasan et al. 2020; Deribew 2020; Shao et al. 2021; Assefa et al. 2021). Prediction and simulation of urban growth and LULC change patterns have become essential to environmental protection and sustainable urban development (Mishra et al. 2021). Furthermore, the urban landscape's complex urban system and structure must be clearly understood to forecast future spatiotemporal urban growth dynamics and LULC changes (Rimal et al. 2018; Rana and Sarkar 2021). In the case of urban growth simulation, the growth processes and historical information must be taken into account to accurately determine spatiotemporal changes and interactions (Gómez et al. 2020 and Alaei et al. 2020), so the process of identifying the fundamental driving factors of urban growth and LULC changes can be realized using simulation techniques (Goncalves et al. 2019). Geographic information system (GIS) and remote sensing (RS) play significant roles in understanding the spatiotemporal dynamics of urban growth and LULC patterns, as well as determining the influential driving factors of these complex urban structures (Liping et al. 2018).

The RS and GIS techniques are widely used to assess and monitor spatiotemporal urban growth dynamics and LULC change patterns (Berila and Isufi 2021). Recently, these techniques have proven to be effective tools for supporting planners and policy makers to develop sustainable policies and make accurate planning decisions. RS and GIS provide many advantages to researchers and urban planners. First, it helps to analyze data spatially and offers various options such as modeling (Akintunde 2019). Second, these techniques provide the interpretation of physical data with socio-economic data, and provide an important linkage in the planning processes (Jat et al. 2017). RS and GIS techniques also help visualization of complex spatial patterns and relationships and help change analysis (Aithal and Ramachandra 2016). These techniques are accessible at a low cost to planners and researchers (Rawat and Kumar 2015). Both effectively monitor, evaluate, analyze, map, and control spatial phenomena (Jat et al. 2017; Aswal et al. 2018). Because of these and other advantages, researchers, urban planners, and policy makers heavily depend on RS and GIS techniques to simulate urban growth patterns and future LULC changes.

Currently, different methods and models utilizing RS and GIS techniques are being applied to model urban growth patterns and forecast LULC changes (Liping et al. 2018). Some studies have used cellular automata (CA)-based Markov chain (MC) models for urban growth modeling (Al-sharif and Pradhan 2014; Abutaleb and Ahmed 2016; Altuwaijri et al. 2019; Aburas et al. 2021), while others applied

quantitative methods like logistic regression to simulate urban growth and LULC changes (Alsharif and Pradhan 2014; Tripathy and Bandopadhyay 2018; Myagmartseren et al. 2020; Salem et al. 2021). Some studies have used the integration of different dynamic simulation and statistical models or hybrid models (Arsanjani et al. 2012; Hamdy et al. 2016; Mozaffaree et al. 2021). For instance, some studies used the integration of CA-based Markov chain (MC) models with logistic regression model to obtain more realistic and appropriate results. Urban growth modeling based on geospatial technologies has been applied to understand better the complex urban growth processes within a specified time. This enables us to develop effective urban growth and land use policies for sustainable urban development and appropriate resource allocation (Hisham et al. 2019).

Integrating cellular automata (CA) models with geographic information system (GIS) introduces a new way of modeling urban growth and LULC changes in a realistic approach, allowing for new possibilities. A robust methodology for monitoring urban complex systems integrates GIS spatial analytical tools with spatial dynamic models such as CA (Mohammadi et al. 2013; Samat 2009). CA model was developed and proposed as an alternative to a pre-existed traditional spatial models in the mid 1988s because of its simplicity, capacity to do dynamic spatial simulations, and capability for producing high-resolution modeling using GIS and remotely sensed data (Maithani 2010a; Fitawok et al. 2020; de Almeida et al. 2003; Blečić et al. 2004). The traditional models such as the concentric zone model and Lowry and Grain-Lowry model were more static and criticized by researchers for being hyper comprehensive, data hungry, and complicated (Maithani 2010a). The ability of the CA model to simulate and predict urban growth patterns and land use changes mainly relies on the assumptions that the previous changes affect the future through local and regional interactions among different land use types (Aburas et al. 2021). The cellular automata (CA) model is highly influenced by cell size, neighborhood type, and size, which have to be considered significant factors while obtaining the best modeling results (S. Q. Wang et al. 2012). CA model is commonly used to model and simulate the changes, dimensions, and trends in urban growth and land use changes (Sang et al. 2011; Aburas et al. 2017). It can be used to analyze and summarize changes in urban and non-urban lands based on the number of transition area probabilities from one status to another status over a specific period (Silver and Silva 2021). MC cannot simulate changes in spatial trends. But it is an effective model to simulate the extent to which land uses have been changed (Azari et al. 2022).

Previous studies have attempted to project the future urban growth and LULC changes in various parts of the world using CA–Markov modeling and determine the factors aggravating it through the application of multi-criteria

evaluation (MCE) and analytic hierarchy process (AHP) techniques. For instance, Jafari et al. (2016) tried to monitor the major land use changes from 1989 to 2013 and forecast the future sprawling of the Hyrcanian region, Iran, for 2023 and 2037 using CA-Markov models. This study revealed that there would be a rapid urban expansion for the target years, with 11,510 ha and 18,320 ha of urban expansion expected, respectively. Tajbakhsh et al. (2016) also examined and modeled urban sprawl and its consequences on the land use land cover changes observed in Mashhad City, Iran. Results of this study on the projected LU maps for the year 2025 indicated that the city's development will be more intense than in the base years. Keshtkar and Voigt (2016) used CA-Markov coupled with the MC model to investigate spatiotemporal landscape changes. This was done to model future landscape changes in the research area of Central Germany from 2020 to 2050. This study found that the continued illegal growth of urban surfaces and radical land use transformation will drastically decline natural resources.

Though they were few, studies were conducted on urban growth in the study area of Bahir Dar. Research by Wubante et al. (2020), for example, attempted to investigate the ecosystem of expropriated land and urban expansion in Bahir Dar City based on sociological research techniques/surveys. Fitawok et al. (2020) used CA-Markov model to forecast the effect of urban expansion on LULC changes in Bahir Dar and simulated the possible LU changes for 2025, 2034, and 2045. However, these studies have shown several limitations. Firstly, these studies have focused on analyzing driving factors over one specified period. This indicates enough attention has not been paid to long-term spatiotemporal dynamics of urban growth and land use change and its driving factors. Second, these studies have failed to incorporate various proximity and physical factors in their model.

Only few factors such as slope and road were considered main driving factors of urban growth processes. These limited independent variable models will lead to biased results and conclusions. But the present study has focused on multiple physical and proximity factors to fill the gaps and solve the problems identified in previous studies. For instance, the study was conducted for long-term study periods (1984–2049), consisting of six study periods and 65 years of spatiotemporal urban growth dynamics in Bahir Dar. But studies conducted before gave much attention to socio-economic factors that drive urban sprawl because of lack of quality data, so more investigations were required to verify the presence of rapid urban growth and model the continued growth trends of the city for the coming year. Though severe environmental and socio-economic problems have resulted from rapid and uncontrolled urban growth in Bahir Dar, previous studies lack to provide detail and critical analysis of these problems, so no study focused on critical analysis of urban growth, driving factors, and future

scenarios until this study was conducted in Bahir Dar. This study was conducted to fill the gaps not covered by previous research in the city and its surroundings.

Previous works indicate a need to forecast and quantify the location and extent of urban growth and LULC changes over time and space. The study area Bahir Dar is chosen for this study because of its fastest growth in recent decades. The urban growth dynamics of the city have not been well documented and adequately analyzed. In addition to its rapid population growth, the city is the hub of socio-economic and political activities of the region in particular and the country in general. This multi-functional nature of the city results in high population and economic flow, which leads to rapid urban growth. In developing countries like Ethiopia, the socio-economic and political conditions may have affected the urban growth, which further leads to rapid and uncontrolled urban growth of cities. The main problem in Bahir Dar is the rapid transformation of land cover types from non-urban to urban landscape, mainly conversion of agricultural fields and forest land to a built-up environment. This is primarily due to the high demand for housing, expansion of transport networks, and industrial and commercial buildings at the expense of agricultural and forest lands. This affects the environment and socio-economic conditions of the city and its surroundings, so this economic transformation and rapid population growth result in unplanned urbanization and change in land use patterns of Bahir Dar City. This problem needs to be evaluated to design an appropriate urban planning system.

The city of Bahir Dar and its surroundings experienced rapid urban growth and fast LULC transformation in the last three and half decades. As a result of this continuous growth, non-urban lands have been converted into urban lands (impervious surfaces), affecting people's livelihood and urban ecology. The current study simulates future urban growth patterns and LULC changes through integrated CA-Markov and MC models in Bahir Dar City, Ethiopia. Firstly, LULC maps of the target years (1984, 1994, 2009, and 2019) were prepared using ArcMap and ERDAS Imagine. Secondly, transitional matrixes were computed from LULC maps using the Markov model to simulate significant changes in the land use/land cover patterns. Thirdly, CA-Markov model have been applied to forecast the spatiotemporal distribution of LU from 2019 to 2049 using a transitional matrix and transitional suitability maps. No study has been conducted on the simulation of urban growth in Bahir Dar and its surroundings using an integrated CA-Markov model for long study periods with multiple variables. The use of high-resolution SPOT satellite images as a reference for LULC mapping provides accurate results and proper conclusions. This study could significantly contribute to plan the future urban growth management in Bahir Dar. It can be an instrument for a decision support system for urban

planners and policy makers to design urban expansion plans with sustainable habitat development.

Methods and materials

Study area

Bahir Dar is a city in Ethiopia's northwest region. It is divided into nine sub-cities and 32 rural kebeles, comprising an area of 213.55 km². The absolute location of the study area lies between 11° 30' 11" latitude and 37° 29' 4" longitude (Fig. 1). The elevation of the study area is ranging from 1117 to 2008 m above sea level. The two most important factors influencing urban growth and land use land cover changes are population growth and economic development (Habibi and Asadi 2011; Lity 2021).

Urban growth in Bahir Dar is occurring mainly due to economic development in the city, rapid growth of population in the outskirts of rural areas, and the political situation of the country in rural areas (Mehriar et al. 2020; Turok and McGranahan 2013). The bad political situation

and maladministration in the rural regions forced the rural community to migrate from rural to urban areas. In addition to this, economic centrality, land use policy, rural–urban migration, socio-political factors, and the process of industrialization are the drivers of the urban growth and LULC changes in the city (Appelhans 2017; Fitawok et al. 2020). As data taken from Ethiopian Central Statistics Agency (CSA) indicated, the research area had a total population of 54,800 in 1984, which increased to 96,140 in 1994, 221,991 in 2007, and 348,429 in 2017. According to the Bahir Dar city administration, the current projected total population of Bahir Dar is 389,177.

Data sets

The Landsat data which was used for this study has been taken from the USGS website <https://earthexplorer.usgs.gov>. These data consist of dry season cloud free Landsat images of thematic mapper (TM) for the years 1984, 1994, and 2009 and operational land imager (OLI) (Table 1 and Fig. 2). All the images used for this study have been freely acquired during the dry seasons from Dec. 24 to April 6 for

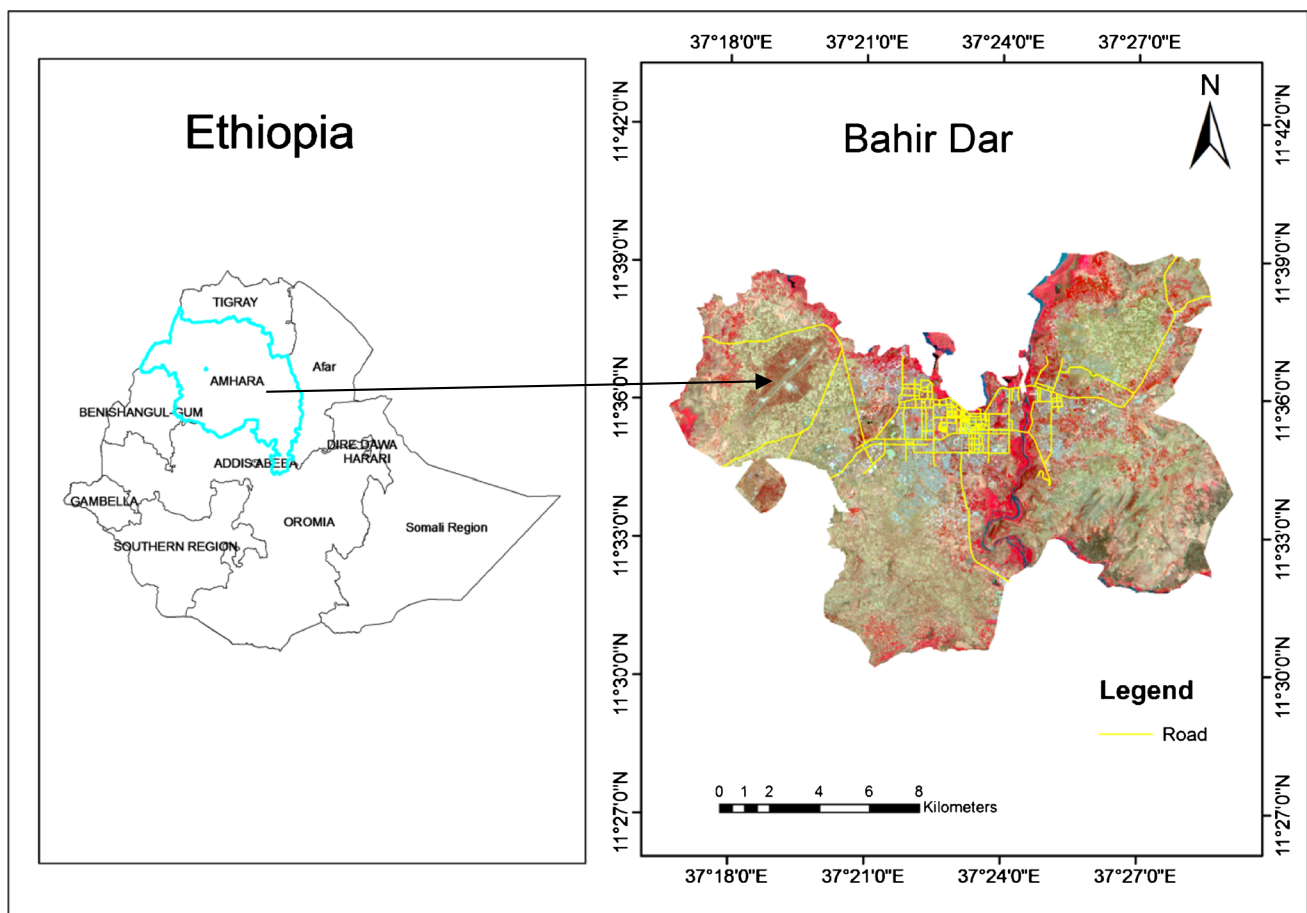


Fig. 1 Study area

Table 1 Data set of Landsat time series images

Study year	Sensors	Satellites	Path/row	Resolution (m)
1984	TM	Landsat 5	170/52	30
1994	TM	Landsat 5	170/52	30
2009	TM	Landsat 5	170/52	30
2019	OLI	Landsat 8	170/52	30

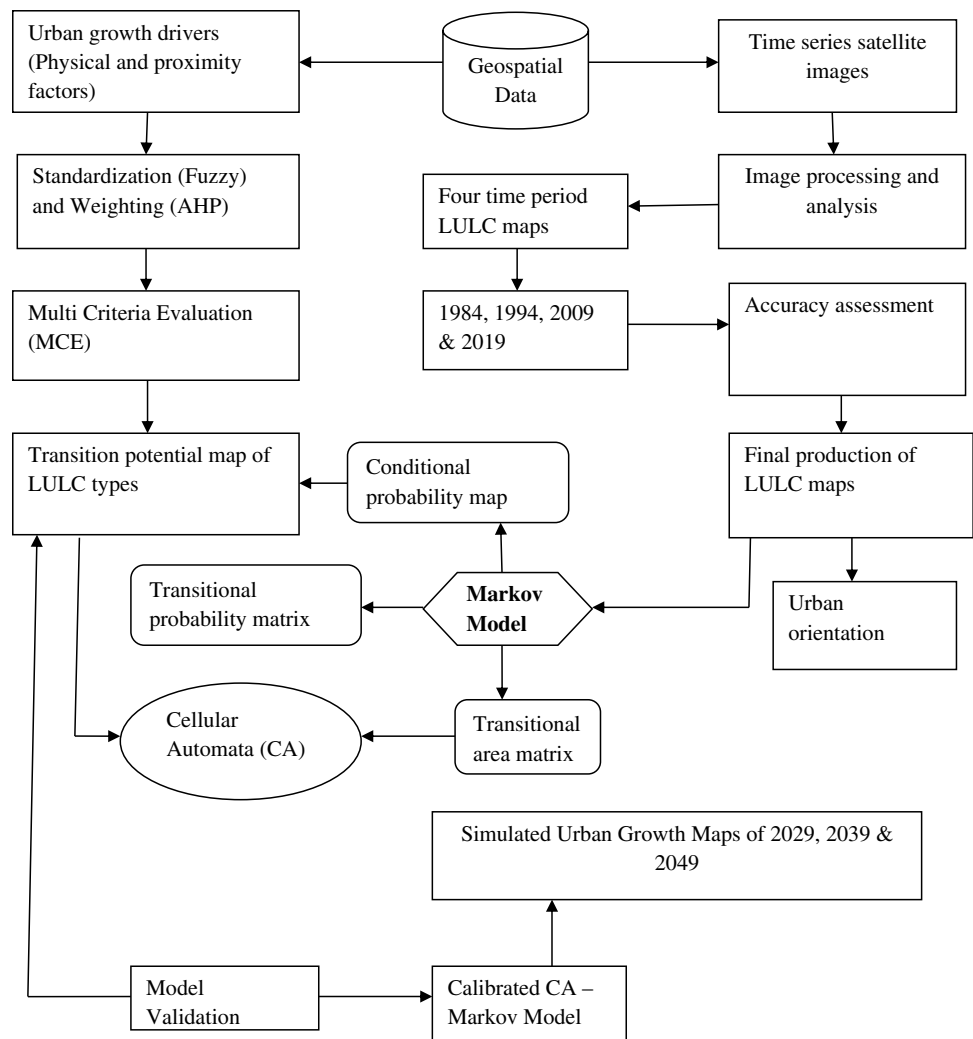
all study years. Furthermore, all the Landsat images and Shuttle Radar Topography Mission digital elevation model (SRTM DEM) with 30-m resolution of the study area were projected in UTM zone 37 N. In addition, the Ethiopian Mapping Agency (EMA) provided high-resolution SPOT 5 and 6/7 images with 1.5 and 5-m resolutions, as well as a topographic map of Bahir Dar for the year 1988 (scale 1: 50, 000) for this study. The administrative boundary vector data covering the research area has been obtained from

the Geospatial Center of Bahir Dar University. The required population data for 1984, 1994, 2007, and 2017 have been collected from Ethiopia’s Central Statistics Agency (CSA). Road network and water body data were taken from Google earth, Open Street Map, and USGS websites.

Pre-processing and classification of images

The satellite imageries have gone subjected to digital analysis. Image pre-processing and various image enhancement techniques such as layer stacking, band composite, and sub-setting and post-processing have been applied on the processed digital data (Fig. 2). In this regard, both radiometric and geometric corrections have been applied to improve the quality of all acquired images. Furthermore, the projection for the satellite imageries was made to the Universal Transverse Mercator projection system, 37 N zone, and datum of world geodetic system WGS84 to ensure the uniformity of the data set during analysis. Arc map 10.3 and ERDAS imagine 2013 were used to pre-process and analyze the data

Fig. 2 Methodological flow-chart



for this study. To apply geometric correction, digital numbers (DN) were converted into spectral radiance and images were processed for radiometric calibration. There are different image enhancement methods to acquire the required information from images. Histogram modification, filtering, and band compositions are some of the methods. The band composition method have been applied in the present study to distinguish the different category information from the image. The false color composite (FCC) of the Landsat images have been used to classify and map the LULC maps. Maximum likelihood supervised classification mechanism was used for image classification and thematic map preparation. Li et al. (2014), Ismail (2009), and Lindström et al. (2006) have used maximum likelihood supervised classification technique for their study. Maximum likelihood supervised classification is more effective and can provide better accuracy. The authors did this classification scheme (Table 2) based on the land use land cover classification method developed by Hassan et al. (2016).

The Landsat images downloaded freely from the USGS website have been directly imported to ArcMap for pre-processing, layer stacking, band composite, and sub-setting. These images were exported from ArcMap for further processing. After that, the exported images were imported to ERDAS image for classification. The authors have taken a total of 360 training points from 6 LULC classes; 60 samples per LULC class were taken randomly. High-resolution SPOT images of 2006 and 2016 have been used as a reference to identify land use classes of 2009 and 2019 and Google maps with a prior knowledge of the researcher. Aerial photo of 1982 and topographic maps of 1984 for Bahir Dar have been used for reference and accuracy assessment of the classified land use map. The map of 1994 was classified and validated using Google earth map, with prior knowledge of the researcher and elder people in the study area. The accuracy for each study period was evaluated using quantitative metrics of overall accuracy and kappa statistics. This accuracy assessment has been evaluated and measured using a stratified sampling approach. The overall accuracy of the land cover maps has been presented as 97.14%, 97.45%, 97.30%, and 97.76%

Table 3 Accuracy assessment results for land use land cover maps

Year	Kappa statistics	Overall accuracy
1984	0.92	97.14
1994	0.89	97.45
2009	0.93	97.30
2019	0.89	94.76

for 1984, 1994, 2009, and 2019, respectively (Table 3). The kappa statistics values for reference years were calculated and the results have been presented as 0.92, 0.89, 0.93, and 0.85 for 1984, 1994, 2009, and 2019, respectively.

Potential driving factors of urban growth

Driving factors of urban growth attracted increasing attention (Guangjin et al. 2016; Liao et al. 2017; Hamdy et al. 2017; Li et al. 2018). According to the literature, various factors are affecting urban growth processes (hinder or promote) such as physical factors (elevation and slope), social factors (population density and social services), environmental factors, political factors (policies), and connectivity factors (distance from road). In this study, distance from the existing urban area, distance from the international airport, distance from forest land, distance from public services, distance from the city center, distance from river, aspect, slope, road distance, and elevation were considered as factors affecting urban growth processes and land use change.

The influence of urban growth factors varies from place to place. So, to select factors of urban growth, an urban planning expert's opinion, interviews with elders, and similar studies carried out by earlier researchers have been used. Population density is crucial for urban growth and land use change because it is directly linked to the urban market, rigid demand, and agglomeration capability (Li et al. 2018; Surya et al. 2020). However, in the present study population density has not been considered as the main driving factor due to insufficient data.

Elevation and slope were usually restrictive factors to urban growth, especially for areas with poor natural conditions and

Table 2 Land cover classification scheme

LULC types	Definition of properties
Built-up	Commercial, industrial, construction and settlement areas, airport, traffic, public services, transport networks, paved and unpaved surfaces, and government secretariat areas
Crop land	Land that is suitable to or used for different types of crop
Forest	An area of land dominated by trees and or land reserved for the growth of forests
Water	Lakes, rivers, ponds, reservoirs
Open space	Land reserved for green area, sport event, recreation, and free non-vegetated areas, which is not allocated for a specified purpose
Wetland	The land found around water bodies such as shrubs, bushes, aquatic vegetations, woodlands, and marshlands

low development (Li et al. 2019). Distance to a river affects urban growth in two ways. First, urban growth is restricted by the presence of rivers/lakes. Second, water resources near the city are an advantage and provide waterborne possibilities that promote urban development into urban fringes (Yanping and Zhen 2019). In Bahir Dar, the presence of Lake Tana and Abay/Blue Nile River has a significant role in urban growth and LULC changes. These characteristics of water bodies and its influence on urban growth do not vary over time.

Distance to a city center is also considered one of the proximity factors. This variable impacts urban growth and land use change through location effects (Kasraian et al. 2019). The closer a region is to the city center, the higher its probability of urban growth. The continuous and rapid urban growth pattern and LULC change in Bahir Dar is the main explanation for this phenomenon because areas near the city center have a high advantage in accessing socio-economic resources with low transport costs. The other potential factor of urban growth and LULC change is distance from the main road, which means transportation accessibility factor or variable characterizing traffic distance of the city. Transportation accessibility factors usually promote urban growth and rapid transformation of land covers. Urban growth along the transport lines (main road) is one of the main urban growth patterns. Transport infrastructure in Bahir Dar has been improved in the last 35 years (1984–2019). This promotes rapid urban growth and LULC change for the last three and half decades and will continue in the future; hence, the CA–Markov model results show these trends.

Pair-wise comparisons of the factors affecting urban growth were conducted to obtain the weight and effect of each driving factor on urban growth processes and LULC change. At first, the matrix of pair-wise comparisons of factors to criteria and criteria to each other is formed and criteria scoring to each other and factors to criteria are performed using an expert in Delphi technique and the field of view. The Expert choice software has been used in the hierarchical analysis process method to calculate each factor’s weight. Others would have its influence on rapid urban growth and LULC change. However, the above factors are the main driving forces of rapid urban growth and land use in Bahir Dar.

Markov chain model and CA Markov

The future trends and spatial structure of urban growth have been modeled using a combination of MC and CA. MC is a quantitative simulation model that can describe urban sprawl dynamics and project future urban growth dynamics depending on transition probability matrix (Maithani 2010b). Cellular automata (CA) are a computational method capable of simulating urban growth processes by describing a complex system through a set of simple rules (Wang et al. 2021). It was designed for urban growth to simulate the process of

urbanization in a hypothetical region. It consists of rules that describe the spatial interaction of cells and the set of parameters that led to the exploration of different urban forms. CA’s ability to simulate urban growth, change land use, and population expansion has become suitable for simulating complex geographical processes (Falah et al. 2020). MC helps predict future land use and provides quantitative information extracted from time series satellite images, which will be used for future urban planning and resource management. It can indicate and explain the probability of changes of land use classes from one to the other based on the information obtained from time series satellite images of two time intervals. Future simulations were done for the coming 30 years in three periods using the proposed model to forecast future LU change and urban growth dynamics depending on LULC classes taken from satellite images (2019–2029, 2029–2039, and 2039–2049). This can also be expressed (Fan et al. 2008):

$$P\left(x_t = \frac{j}{x_0} = I_0, X_1 = i_1, \dots, X_{t-1} = i_{t-1}\right) = P(x_t = \frac{j}{X_{t-1}} = i_{t-1}) \tag{1}$$

If a Markov sequence of random variant takes the discrete value a_1, \dots, a_n , then:

$$P\left(x_n = \frac{a_{in}}{x_{n-1}} = a_{i_{n-1}} \dots, X_1 = a_{i_{n-1}}\right) = P(x_n = \frac{a_{in}}{a_{i_{n-1}}}) \tag{2}$$

where P is the transitional probability matrix, x_t is the state of cell x at time t , X_{t-1} is the state of cell x at earlier time, and i_{t-1} refers to the state of cell i at earlier time. The sequence x_n is named a Markov chain. The CA–Markov model has the advantage of providing a good projection of spatiotemporal LULC changes and urban growth changes in quantity and space (Parsa and Salehi 2016). CA uses a bottom-up approach, making it more appropriate to incorporate temporal and spatial components in given processes (Santéet al. 2010; Rimal et al. 2017). A discrete grid dynamic system characterizes this model with regular divided spatial cells and time progresses in discrete steps. It updates the state of each cell using local rules; the state of each cell at a given time is determined by the state of its own and its neighbors at the previous time step (Torrens 2001). The results of the investigations reported by Liu et al. (2021), Liu and He (2009), Helbich and Leitner (2009), Triantakoustantis and Mountarakis (2012), Halmy et al. (2015), and Waseem et al. (2017) confirm that the integration of MC–CA models, multi-criteria evaluation (MCE), and AHP are the most fundamental decision-making operations and enable the evaluation of group decisions systematically and logically. Previous studies have used cellular automata-based Markov chain model to simulate the future spatiotemporal dynamics of urban growth and land use change pattern. For instance, Samat et al. (2011)

used CA model to simulate the land use changes at peri-urban areas of Perai region, Penang State, Malaysia. This study applied the cellular automata modeling using the Land Change Modeler module of IDRISI Selva software. It reveals that all the approaches used in this model are very simple and can easily be implemented to foresee the future spatial pattern of urban growth using different policy approaches.

Study by Zhu et al. (2021) used cellular automata to simulate urban land use change with a constraint irregular space representation in Nanjing City, China. The study applied this model in the same application used by previous research (IDIRISI software) to simulate the land use changes. Mozaffaree et al. (2021) used cellular automata model for simulation of urban expansion in Tallinn, Estonia. All the necessary data were processed in ArcGIS and then the CA modeling was applied in IDRISI Selva Land Change Modeler module. The other study carried out by Falah et al. (2020) used CA and AHP to model urban growth in Qazvin City, Iran. This study detects the extent of urban sprawl using Shannon's entropy through remote sensing and GIS. Simulation of future growth of the city was done using the IDRISI Selva software.

The LULC maps were input for CA-Markov models. The LULC maps prepared in the ERDAS software were imported to the IDRISI Selva software and land use maps (earlier and later) were processed using the Land Change Modeler module to harmonize the different map elements. The conditional transition images were created using a Markovian transition estimator from the earlier (2009) and later (2019) images/LULC maps. The simulation used CA-Markov models based on Markov transition area files and transition suitability image collections. The land use map of 2019 was used as base year and starting point to predict the urban growth of Bahir Dar for the upcoming 30 years. The general steps implemented in the IDRISI Selva software to apply CA-MC models are the following: (1) construction of CA-Markov suitability maps; (2) generation of the transfer matrix and the state of transitional probability matrix using Markov model; and (3) production of future land use using CA. In this study, the transition probability/potential matrix was derived from the land use conditions in 1984–1994, 1994–200, 2009–2029, and 1984–2019, so the urban growth map of 2019 was used as a reference map to simulate 2029, 2039, and 2049 by computing the matrix transitional areas. The mapping and analysis were conducted using ArcGIS 10.3, ERDAS Imagine 2013, and IDRISI Selva 17.0 (Table 4).

Analytical hierarchy processes

Analytical hierarchy processes (AHP) are multi-criterion decision-making techniques (Saaty 1987). It provides a thorough and rational framework for making

Table 4 AHP evaluation scale (Saaty 1987)

Intensity of importance	Definition
1	Equal importance
3	Moderate importance
5	Essential/strong importance
7	Very strong importance
9	Absolute/extreme importance
2–4 and 6–8	Intermediate importance
1/3, 1/5, 1/7	Values for inverse comparison

decisions and comparing alternatives (Waseem et al. 2017). AHP is utilized to compute the weight of variable maps which pass through fuzzy standardization processes in the IDRISI Selva software using pair-wise comparison of factors involved in urban growth processes (Table 5). It also gives the decision-maker more options (Ozdemir and Saaty 2006). There are steps to AHP modeling: (1) structuring the hierarchy. AHP entails defining the problem from top to bottom, deciding on criteria, and developing alternatives (Saaty 1987). Second (2) is computing decision matrix and pair-wise comparisons. This phase compares a factor at one level to another at the higher level in the hierarchy. The weights of maps used for identifying the influential factors of urban growth and LULC changes are computed using weights given to criteria. The formulas below were used to calculate the weight of the criteria (Mohammadizadeh et al. 2016):

- Prepare a (nxn) pair-wise comparison matrix for multiple factors. It is proposed that a_{ij} = the chosen factor (factor i to factor j). Then, $a_{ij} = 1/a_{ji}$ was assumed.
- For this calculation, the matrix values are normalized, and a sum of each column is computed. Each binary comparison element is divided by the total value of the column in which it is located. The normalized comparison matrix values were obtained using these calculation procedures.
- The mean values of each row in normalized comparison matrix are determined. These averages represent an estimate of relative priorities for the compared elements.
- Finally, the consistency ratio is checked. Each matrix's eigenvectors and maximum eigenvalue were computed. Then, the consistency index is then using the procedures below.

$$CR = \frac{\lambda_{\max} - n}{n - 1} \quad (3)$$

where λ_{\max} represents the eigenvalue of the paired comparison matrix.

Table 5 Pair-wise comparison matrix generated from AHP

	DRD	SLP	DCC	DBU	DAPT	ELN	DPS	DR	DF	AST	Weights
DRD	1										0.294
SLP	1/2	1									0.215
DCC	1/3	1/2	1								0.154
DBU	1/4	1/3	1/2	1							0.109
DAPT	1/5	1/4	1/3	1/2	1						0.076
ELN	1/6	1/5	1/4	1/3	1/2	1					0.054
DPS	1/7	1/6	1/5	1/4	1/3	1/2	1				0.038
DR	1/8	1/7	1/6	1/5	1/4	1/3	1/2	1			0.027
DF	1/9	1/8	1/7	1/6	1/5	1/4	1/3	1/2	1		0.019
AST	1/9	1/9	1/8	1/7	1/6	1/5	1/4	1/3	1/2	1	0.010

*DRD distance from main road, SLP slope, DCC distance from city center, DBU distance from existing built-up area, DART distance from airport, ELN elevation, DPS distance from public services, DR distance from river, DF distance from forest, ASP aspect

The consistency ratio (CR) of the paired comparison matrix was tested as follows:

$$CR = CI/R \tag{4}$$

where RI is the random consistency index.

A valid CR has a value of 0.10 or 10% or less. A CR value greater than 0.10 indicates the AHP process needs a regenerated pair-wise comparison matrix (Saaty 1987). The pair-wise comparison process was repeatedly done until the CR < 0.1 value was obtained.

Previous studies identified various factors responsible for urban growth in different urban centers. These factors could have a different level of influence over space and time, so to minimize the limitations regarding this variation, the researcher selected the factors in a very wise and careful way. First, the researcher selected 15 factors of urban growth and land use change from previous literatures. Then, interview was conducted with local experts and elder people about the factors. Among the 15 factors, five factors were removed from analysis based on the data availability and context of the study area by urban planning experts. Factors removed from this study were population density, land value, GDP, proximity to railway, and proximity to the nearby satellite towns. In this study, the pair-wise comparison of the relative importance of the variables is compared using Saaty’s 1–9 scale in the IDRISI software (Table 4), so expert knowledge in the area resulted selection of 10 factors for this study. The researcher prepared pair-wise comparison questionnaires for 12 local urban planning experts. Based on the response of these experts, the researcher computed the weights of urban growth factors using AHP in IDRISI, so the relative

importance of factors was determined by the values given by experts. Furthermore, the consistency ratio (CR) is used to check the accuracy of the values assigned to the factors by experts. In this study, the researcher applied a 10*10 pair-wise comparison matrix to determine and generate the weight of the selected factors using AHP in the IDRISI software (Table 5).

CA–Markov validation approach

The overall achievement rate was determined by kappa index calculations, which allows for a better understanding of the key determinants of weakness and strength of results. The maps generated for the study are in a high level of agreement when $75\% \leq \text{kappa} < 100$; they are in a medium level of agreement when $50\% \leq \text{kappa} \leq 75\%$; and they are in a poor agreement when kappa is below 50% (Pontius 2000; Pontius et al. 2001), so the model was validated to verify the accuracy of the CA–MC simulation model to project the condition of the future LULC of the study area (Omar et al. 2014) following 2019 land use simulations using 1994 and 2009 classified images. Kappa index of agreement (K_{IA}) (Mosammam et al. 2017) includes kappa for location (k_{location}), kappa for standard (k_{standard}), kappa for no information (K_{no}), and kappa for strata (k_{strata}). Mosammam et al. (2017) and Omar et al. (2014) assess the level of agreement between the projected and actual LU maps using the validation module in IDRISI. The validated model was also used to compare the area of the actual and simulated land use maps of the research area. The kappa index values for this model are acceptable (> 75%), so predicted land cover maps of 2029, 2039, and 2949 are valid. As stated by Omar et al.

(2014), kappa statistics can be calculated using the following equations:

$$\text{Kappa for no information} = \frac{M(m)N(n)}{P(p) - N(n)} \quad (5)$$

$$\text{Kappa for location} = K_{\text{location}} = \frac{M(m) * N(n)}{P(m) - N(n)} \quad (6)$$

$$\text{Kappa for quantity} = K_{\text{quantity}} = \frac{M(m) * H(m)}{K(m) - H(m)} \quad (7)$$

$$\text{Kappa standard} = K_{\text{standard}} = \frac{M(m) * N(n)}{P(p) - N(n)} \quad (8)$$

where K index refers to k_{no} , K_{location} , and k_{standard} , and no information is defined by $N(n)$, medium grid cell level by $M(m)$, and perfect grid cell level information across the landscape by $P(p)$.

Analysis and result

Land use/cover structure changes

For the study period (1984–2049), the classification of land use (Figs. 3, 4, 5) employed in the model that is proposed consists of six classes, as determined by spatial overlay analysis in a GIS environment: wetlands, water bodies, open space, forest, crop land, and built-up land (Table 2). Built-up (urban) area increased from 243.94 to 2529.98 ha from 1984 to 2019, and urban development has increased by 2285.06 ha in the last 35 years. However, during this period, crop land was decreased by 11.17% from 1984 to 2019. In the same study period, forest land was reduced by 2.69% due to increasing trends of artificial surfaces/constructions (Table 6, 7, 8, 9).

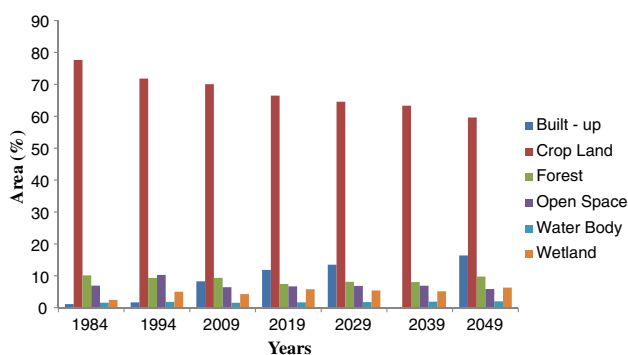


Fig. 3 Area of LU/LC classes of Bahir Dar in percentage in 1984, 1994, 2009, 2019, 2029, 2039, and 2049

Based on the CA–Markov modeling results, the built-up area will continue increasing in its expansion from 2529.98 ha (Table 5) in 1984 to 3983 ha (Table 11). This indicates that the built-up area will increase by 18.56% from 2019 to 2029 at the expense of crop land, forest, and open spaces (Fig. 3), whereas crop land will continue declining because of the rapid growth of built-up surfaces towards these land covers. Forest land will reduce from 1589.39 ha in 2019 (Table 5) to 638 ha in 2029 (Table 11). The figure above (Fig. 3) indicates that built-up will continue to increase in the next 30 years (2029–2049) from 2598.98 to 4998 ha. However, crop land will decline from 14,183.2 to 12,736 ha due to rapid urban growth towards agricultural fields of urban fringes, green areas, and open spaces (Fig. 3).

Evaluating the accuracy and validation of land use maps is the most important aspect of land use classification, land use change detection, and modeling. The classification accuracy for land use land cover maps was calculated and evaluated using statistics like kappa coefficient, producer's, user's, and overall accuracy. Overall classification accuracy is the percentage of correctly classified samples of an error matrix. It is computed by dividing the total number of correctly classified samples by the total number of reference samples. The kappa coefficient is a measure of the overall agreement of a matrix. In contrast to the overall accuracy — the ratio of the sum of diagonal values to total number of cell counts in the matrix. The kappa statistics coefficient which ranges from -1 to $+1$ shows the degree of accuracy of the base map/reference data and LULC values of the classified images (Congalton 2001). A kappa coefficient less than zero indicates that there is less agreement; $0-0.2$ means slight agreement; $0.2-0.41$ shows fair agreement; $0.41-0.60$ means moderate agreement; $0.61-0.80$ means substantial agreement and $0.81-1.0$ perfect agreement. The overall classification accuracy for 1984, 1994, 2009, and 2019 were 97.14%, 97.45%, 97.3%, and 94.76%, respectively, while the kappa statistics values for the stated years were 0.92, 0.89, 0.85, and 0.89, respectively (Table 3).

LULC conversions analysis

In the current study, the conversion of LULC from one class to the other class all over the study periods has been depicted (Tables 7, 8, 9). Persistence is represented by the diagonals of the matrix from the tables, whereas conversions from one category to another are represented by the off-diagonals (Table 7). Between 1984 and 1994, 149.5, 843.9, 584.8, 10.1, and 16 ha of land have been transformed from built-up, forest, open space, water, and wetland, respectively, to crop land, though large amount of crop land was persisted and continued as an agricultural field (Table 7). During this study period, 213.7, 37.7, 17.9, 7.9, and 3 ha of land were converted from crop land, forest, open space, water body,

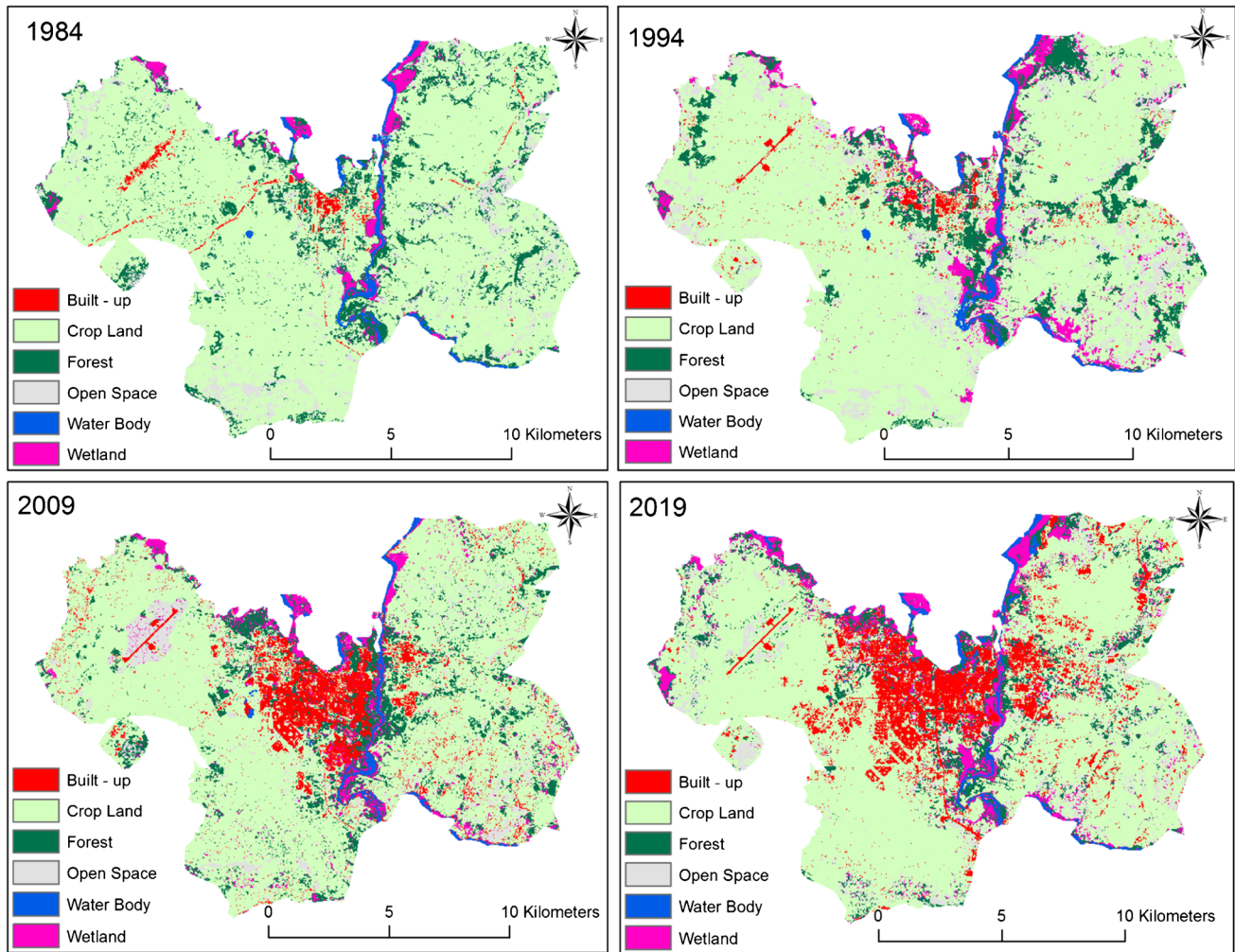


Fig. 4 Land use land cover map of Bahir Dar for the years 1984, 1994, 2009, and 2019

and wetland to built-up. At the same time, 77.5 ha of built-up area persisted and continued as built-up land during this time. As indicated in the table below (Table 7), the conversion of water body (10.1 ha) and built-up (149.5 ha) to crop land was high. There are different reasons responsible for these transformations of water bodies and built-up land. Due to deforestation and overgrazing, water bodies have been changing to dry land in Ethiopia, so this could happen because of this high land use transformation and rapid urban growth. In the case of built-up land, farmers in the surrounding areas/urban fringes are displaced from their dwellings and migrated to Bahir Dar and other small towns due to government plans of redevelopment and provision of land to investors, so built-up land in urban fringes was replaced by large private and government investments. The other reason could be the seasons by which the Landsat images were captured. Dry season images were used for this study, so built-up and crop lands may have similar reflections during harvesting seasons.

Between 1994 and 2009, 122.7 ha, 969.6 ha, 1301 ha, and 436 ha of land were changed from built-up, forest, open space, and wetland to crop land, respectively. In the same period, a large amount of crop land was converted to other land use classes, i.e., 1067.3 ha to built-up, 1030 ha forest, 998.9 ha to open space, and 244.3 ha to wetland (Table 8).

Between 2009 and 2019, a high rate of conversion was observed in built-up and crop land because of rapid urban expansion at the expanse of the other land uses, mainly crop land. During this period, 1122.3 ha, 188.6 ha, 78.6 ha, 7.9 ha, and 55.5 ha of land have been converted from crop land, forest, open space, water body, and wetland to built-up, respectively, even though, built-up was also converted into other land use categories; crop land (511.2 ha), forest (91 ha), open space (44.7 ha), and wetland (102.3 ha).

Fig. 5 Driving factors for CA–Markov model. **a** Distance from road. **b** Slope map. **c** Distance from city center. **d** Distance from built-up areas. **e** Distance from airport. **f** Elevation. **g** Distance from public services. **h** Distance from river. **i** Aspect. **j** Distance from forest

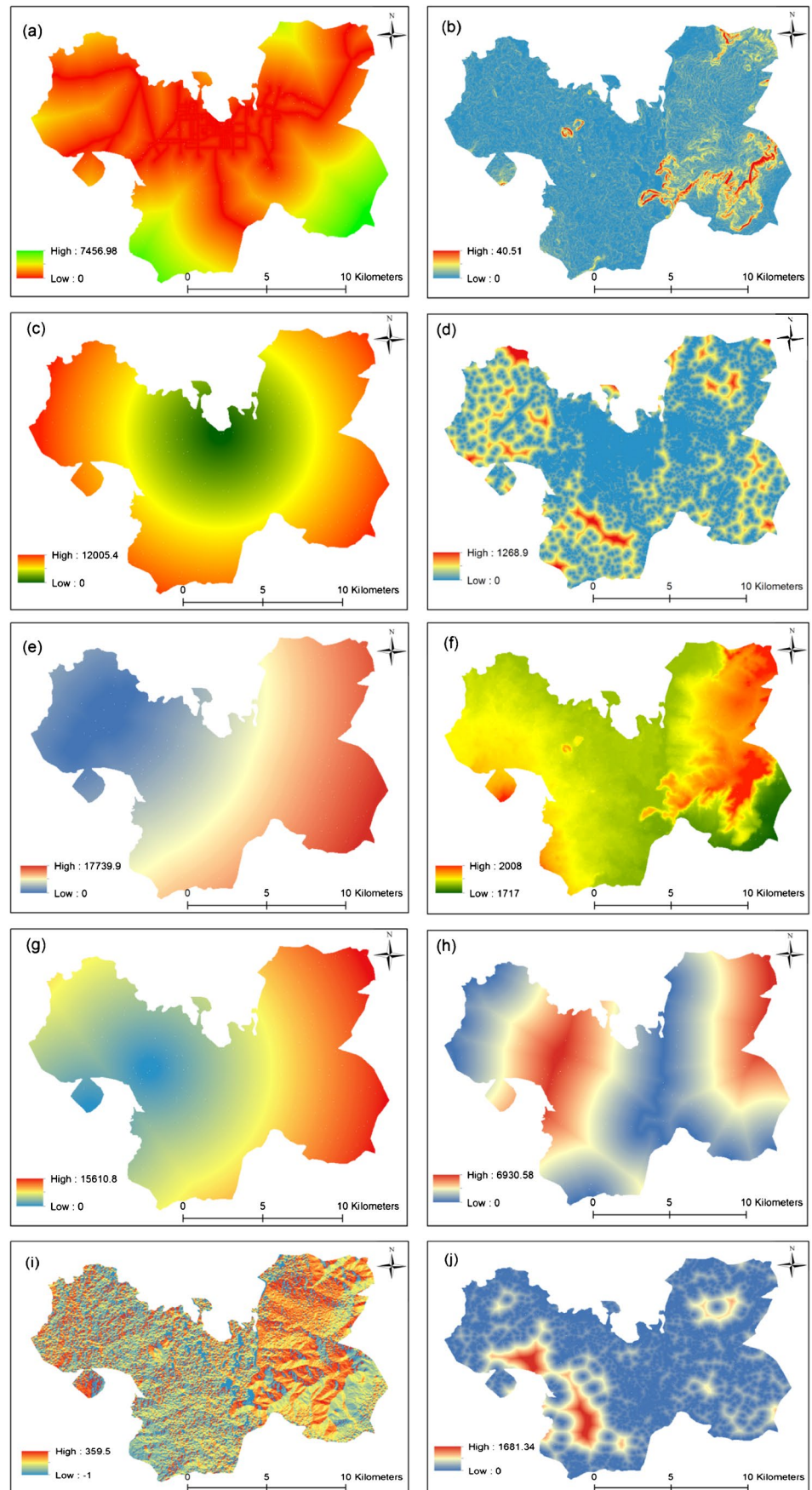


Table 6 Percentage changes of the area of land use classes over the study period

Land use classes	Changes in land use classes (%)							
	1984		1994		2009		2019	
	Area (ha)	%	Area (ha)	%	Area (ha)	%	Area (ha)	%
Built-up	243.94	1.14	357.56	1.68	1768.09	8.29	2529.98	11.9
Crop land	16,568.1	77.66	15,319.8	71.82	14,947.8	70.07	14,183.2	66.5
Forest	2163.95	10.14	1993.85	9.35	1998.68	9.37	1589.39	7.45
Open space	1478.74	6.93	2196.13	10.29	1371.67	6.43	1428.98	6.7
Water body	356.98	1.57	392.66	1.84	332.22	1.56	361.05	1.69
Wetland	523.13	2.45	1071.93	5.02	913.68	4.28	1239.12	5.81

Table 7 Transition area matrix between the study year 1984 and 1994

Land use classes		Land class 1994						Grand total
		Built-up	Crop Land	Forest	Open Space	Water Body	Wetland	
Land class 1984	Built - up	77.5	149.5	7	5.6	1.1	2.7	243.4
	Crop Land	213.7	13709	930.3	5.6	29.7	287.9	15176.2
	Forest	37.7	843.9	587.6	5.6	39.7	332.8	1847.3
	Open Space	17.9	584.8	305.6	5.6	0.7	105	1019.6
	Water Body	7.9	10.1	5.6	5.6	310.1	20	359.3
	Wetland	3	16	152.5	5.6	10	317	504.1
	Grand total	357.7	15313.3	1988.6	5.6	391.3	1065.4	19121.9

Table 8 Transition area matrix between 1994 and 2009

Land use classes		Land class 2009						Grand total
		Built-up	Crop Land	Forest	Open space	Water Body	Wetland	
Land class 1994	Built-up	170.4	122.7	32.2	17.5	2.8	11.1	356.7
	Crop Land	1067.3	11958.5	1030	998.9	12.7	244.3	15311.7
	Forest	288.7	969.6	400.2	94.3	4.9	230.6	1988.3
	Open Space	164.6	1301	337.9	276	0.4	94.2	2174.1
	Water Body	31.2	11.9	7.4	1.7	293.4	45.4	391
	Wetland	120	436.1	181.9	22	16.5	288.1	1064.6
	Grand total	1842.2	14799.8	1989.6	1410.4	330.7	913.7	21286.4

Determined driving factors for urban growth and LULC changes

Several factors are considered driving forces of rapid urban growth and speedy LULC changes for this research. Distance from the existing urban area, distance from the international airport, distance from forest land, distance from public services, distance from city center, distance from river, aspect, slope, road distance, and elevation were taken into consideration as driving factors; see Fig. 8, processed in ArcMap and IDRISI selva for urban growth projection.

These criteria were chosen from the preliminary investigations’ expert conclusions (Lawal et al. 2011; Arsanjani et al. 2012; Hamdy et al. 2016). Here consistency ratio (CR) of the weights specified was determined to ensure their logical consistency, and a result of $CR \leq 0.1$ reveals the correctness of the matrix (Table 10).

In the case of weight of variables determining urban expansion in Bahir Dar, distance from road, slope, distance from CBD, distance from built-up, and distance from airport are most effective driving factors with final weight of 0.29, 0.21, 0.15, 0.10, and 0.076, respectively (Table 10).

Table 9 Transition area matrix between 2009 and 2019

Land use classes		Land class 2019					Grand total	
		Built -up	Crop Land	Forest	Open space	Water Body		Wetland
Land class 2009	Built -up	1072.8	511.2	91	44.7	18.6	102.3	1840.6
	Crop Land	1122.3	11600.7	649.3	865.3	42.8	510.4	14790.8
	Forest	188.6	709.4	601.6	255.6	12.3	220.5	1988
	Open space	78.2	1120.7	27.7	169.5	0	12.9	1409
	Water Body	7.9	18.8	11.4	0.03	229.3	62.3	329.73
	Wetland	55.5	196.6	200.2	84.3	55.4	320.3	912.3
	Grand total	2525.3	14157.4	1581.2	1419.43	358.4	1228.7	21270.43

Table 10 Fuzzy model standardization of variables and its weights extracted from analytical hierarchy processes (AHP)

Factors	Shapes	Weight
Distance from road (m)	J-shaped	0.294
Slope (%)	Sigmoidal/decreasing	0.215
Distance from city center (m)	Linear/increasing	0.154
Distance from built-up (m)	Linear/increasing	0.109
Distance from airport (m)	Linear/increasing	0.076
Elevation (m)	Sigmoidal//decreasing	0.054
Distance from public services (m)	Linear/increasing	0.038
distance from river (m)	Linear/increasing	0.027
Distance from forest (m)	Linear/increasing	0.019
Aspect (°)	Sigmoidal/decreasing	0.010
Consistency ratio (CR)		0.041

The other variables used in the model, such as elevation, distance from public services, distance from river, and distance from water body and aspect, have insignificant

influence over the rapid growth and land use transformation into the other land use categories in Bahir Dar.

Distance from the main road (Addis Ababa to Gondar and Dessie town) plays a significant role in Bahir Dar’s growth. The city has been growing along this road and areas close to this transport line have better accessibility to socio-economic and political services. Urban areas with a distance of 0–1316 m from the main road have the highest chance of urban development. Urban areas with a distance of 1316–3392 m from the main road have medium growth opportunities. However, areas > 3392 m distance from the main road have no probability of growth/are not suitable for development.

The other main driving factor of urban growth and LULC change in Bahir Dar is the slope. Urban areas located in Bahir Dar with a 0% slope have the highest suitability for urban growth and parts of the city with 0–13% have decreasing urban growth suitability. However, areas with > 13% have no suitability for urban growth. This means urban areas with a slope > 13% restricts urban growth or demand a high cost of urban development.

Table 11 Markov transition probability matrix calculated using LULC maps of 1984–1994

Changing from:	Probability of changing by 1994 to:						
1984	Wetland	forest	Open space	Crop Land	Water Body	Built -up	Total
Wetland	0.5112	0.3703	0.0535	0.0374	0.0190	0.0086	1
Forest	0.1679	0.2303	0.1546	0.4110	0.0174	0.0188	1
Open space	0.0760	0.2135	0.2653	0.4319	0.0004	0.0129	1
Crop Land	0.0305	0.0935	0.1476	0.6998	0.0033	0.0254	1
Water Body	0.1093	0.0240	0.0084	0.0643	0.7459	0.0481	1
Built -up	0.0114	0.0313	0.0268	0.6630	0.0059	0.2617	1
Total	0.9063	0.9629	0.6562	2.3074	0.7919	0.3755	6

Distance from the center of the city is also a potential factor that affects urban growth and LULC change in Bahir Dar. It is the main attraction point/growth pole of the city and its surroundings. According to this study, areas closer to the city center have the highest likelihood of urban growth than the urban fringes. Accordingly, areas of the city located 0–4614 m have the highest probability of urban growth, or such distance from the city center promotes urban growth. In contrast, areas found from 4614–7674 m have a decreasing probability of urban growth compared to regions of the city closer to the city center. In contradiction, parts of the city located at a distance > 7674 m are not suitable for urban growth.

Based on this study, distance from built-up areas is also the main driving factor of urban growth and land use change in Bahir Dar. Distance of 0–149 m from existing built-up areas promotes urban growth, while distance 149–373 m decreases urban development probability. Areas > 373 m have no probability of urban growth or are not suitable for urban development due to a high distance from existing urban patches.

According to the findings of this study, the other factors selected and included for this study have no significant role in urban growth in Bahir Dar. This is determined based on their weights extracted from the analytical hierarchy processes (AHP). These variables have a weight below 0.1, which is a low value to consider as the main driving forces of urban growth and LULC change in the study area (Table 9).

Markov chain transition matrix

The table (Table 11) reveals the Markov chain probability matrix summary for major LULC transitions in Bahir Dar between 1984 and 1994 and the possible quantity in the projection of future LULC changes observed from different land categories. For instance, Table 10 shows 51.12% transition

probability of wetland to wetland is 51.12%, whereas the future transition probability of wetland to forest was 37.03%. The transition probability of crop land to crop land was 69.99%, whereas from crop land to built-up was declined to 2.54%. Between 1994 and 2009, the future transition probability of crop land to crop land is 68.38% and from built-up to built-up is 70.2%. At the same time, the future transition probability of crop land to built-up is 7.2%. In the third period (2009 to 2019), the future transition probability of cropland to cropland was 84.86% and for built-up to built-up is 84.99%. The other LULC classes had less probability remaining as they are. However, the probability of the future transition of crop land to built-up was expected to be 25.4%, followed by forest (18.8%) and open space (12.9) from 1984 to 1994. Table 12 shows 57.4 transition probability of wetland to built-up, followed by crop land to built-up (15.79%) and water body to built-up (12.7%) from 1994 to 2009. In the third study period (2009–2019), forest land has a high transition probability (87.79%) to built-up, followed by crop land (15.7%) and water body (12.7%). In general, the probability matrix tables (Tables 11–13) show the growing and decreasing probability of changing land use over time.

Cellular automata-based Markov chain modeling

This type of modeling was used to calculate the area of the anticipated urban growth and LULC types for 2029, 2039, and 2049, as shown in the figures below (Figs. 6, 7, 8). For this study, built-up and cropland showed significant changes compared to the other land use land cover types (Tables 14, 15 and 16). For instance, cropland was decreased from 13,787 ha in 2029 to 13,526 ha in 2039 and 13,556 ha in 2039 to 12,736 ha in 2049, respectively. A continuous increase in the built-up area will be observed in 2029 3938 ha (18.61%), 2039 4214 ha (19.69%), and 2049

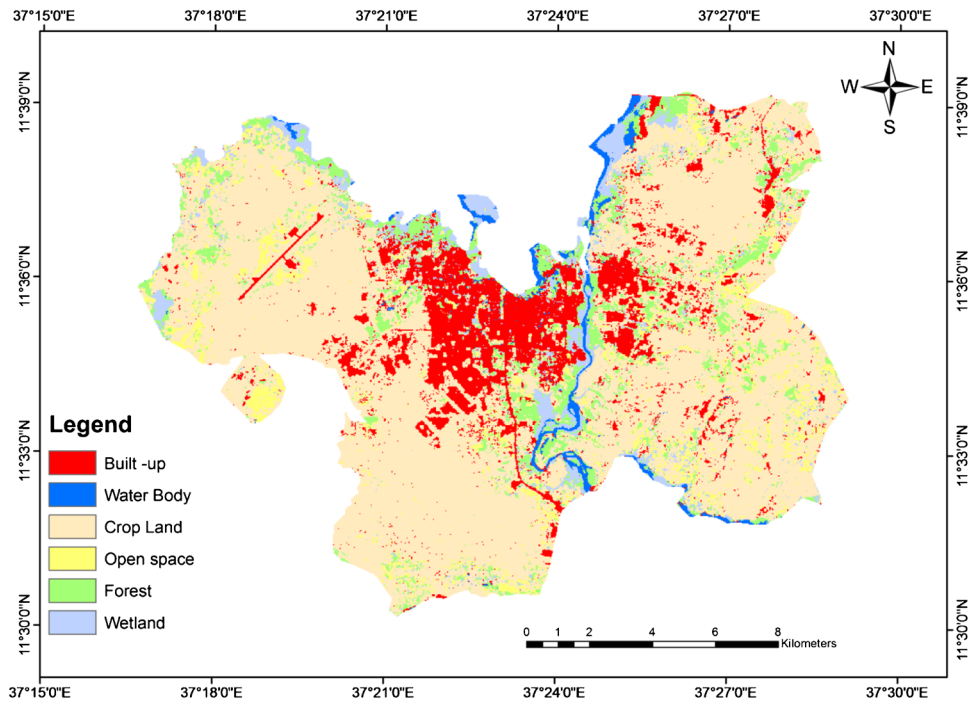
Table 12 Markov transition probability matrix calculated using LULC maps of 1994–2009

Changing from:	Probability of changing by 2009 to:						
1994	Wetland	forest	Open space	Crop Land	Water Body	Built -up	Total
Wetland	0.5443	0.2206	0.0551	0.0966	0.0261	0.0574	1
Forest	0.2158	0.3493	0.0930	0.2375	0.0040	0.1004	1
Open space	0.0085	0.0188	0.2899	0.6420	0.0000	0.0408	1
Crop Land	0.0423	0.0418	0.1547	0.6838	0.0047	0.0728	1
Water Body	0.3056	0.0233	0.0030	0.0353	0.6129	0.0199	1
Built -up	0.0418	0.0188	0.0117	0.2157	0.0099	0.7020	1
Total	1.1583	0.6726	0.6074	1.9109	0.6576	0.9933	6

Table 13 Markov transition probability matrix calculated using LULC maps of 2009–2019

Changing from:	Probability of changing by 2019 to:						
2009	Wetland	forest	Open space	Crop Land	Water Body	Built -up	Total
Wetland	0.8056	0.1520	0.0000	0.0000	0.0424	0.0000	1
Forest	0.0598	0.8371	0.0008	0.0000	0.0145	0.0879	1
Open space	0.0101	0.1411	0.8447	0.0000	0.0000	0.0041	1
Crop Land	0.0000	0.0026	0.0000	0.8402	0.0000	0.1571	1
Water Body	0.0243	0.0000	0.0000	0.0000	0.8486	0.1271	1
Built -up	0.0000	0.0000	0.0000	0.0000	0.1501	0.8499	1
Total	0.8998	1.1328	0.8455	0.8402	1.0556	1.2261	6

Fig. 6 Projected 2029



4998 ha (23.35%), respectively. Water bodies, on the other hand, will show a nearly consistent proportion from 2029 (1.77%) to 2039 (1.91%) and 2049 (2.01%). This figure will be insignificant for the LULC changes of the study area in the projected years. Built-up areas are predicted to expand at the expense of other LU types, specifically cropland.

Model validation and calibration

It is obvious that quantitative models that are applied to simulate the future condition of natural and artificial land could pass through a validation process to ensure the degree of validity and verify the results obtained from it. Likewise,

for validation of the proposed model, the actual (a) and projected (b) (Fig. 9) LULC maps for 2019 were compared and the *k* coefficient for quantity and location was calculated (Fig. 10 and Table 15). The statistical result obtained in these model validation shows that k_{no} is 0.8816, $k_{location}$ is 0.8899, $k_{locationstrata}$ is 0.8799, and $k_{standard}$ is 0.8483, respectively (Table 15). These figures reveal that the quantification and location errors are almost nonexistent or minor. This shows that the simulation can accurately specify both location and quantity. All the *k* index values are greater than 80%, indicating a strong agreement between the actual and projected LULC maps for 2019. The *k* statistics further show

Fig. 7 Projected 2039

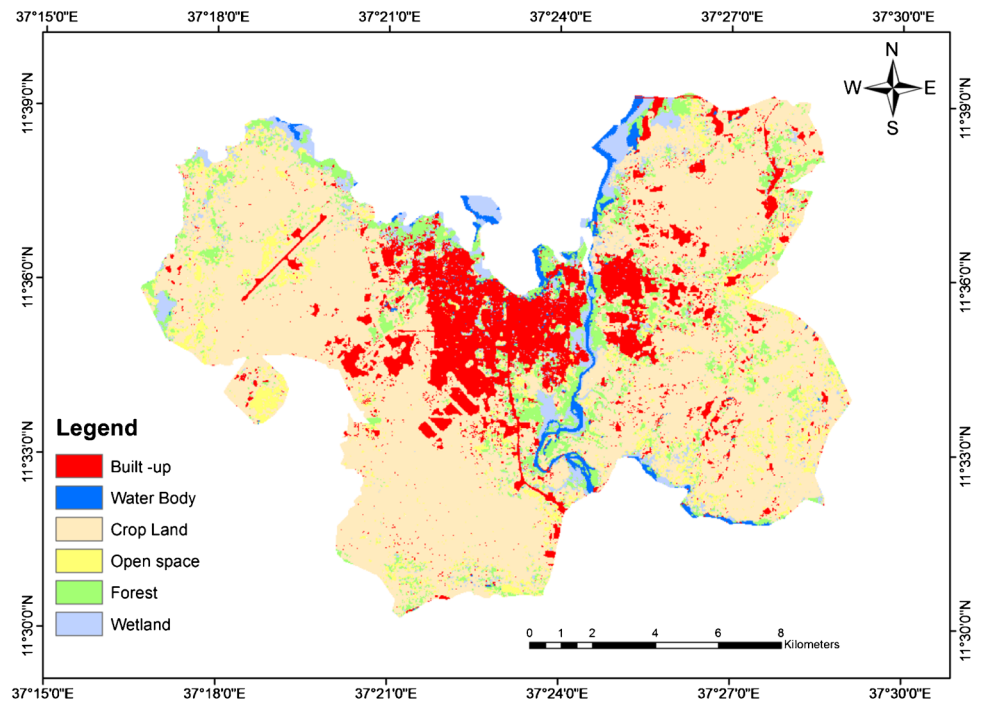


Fig. 8 Projected 2049

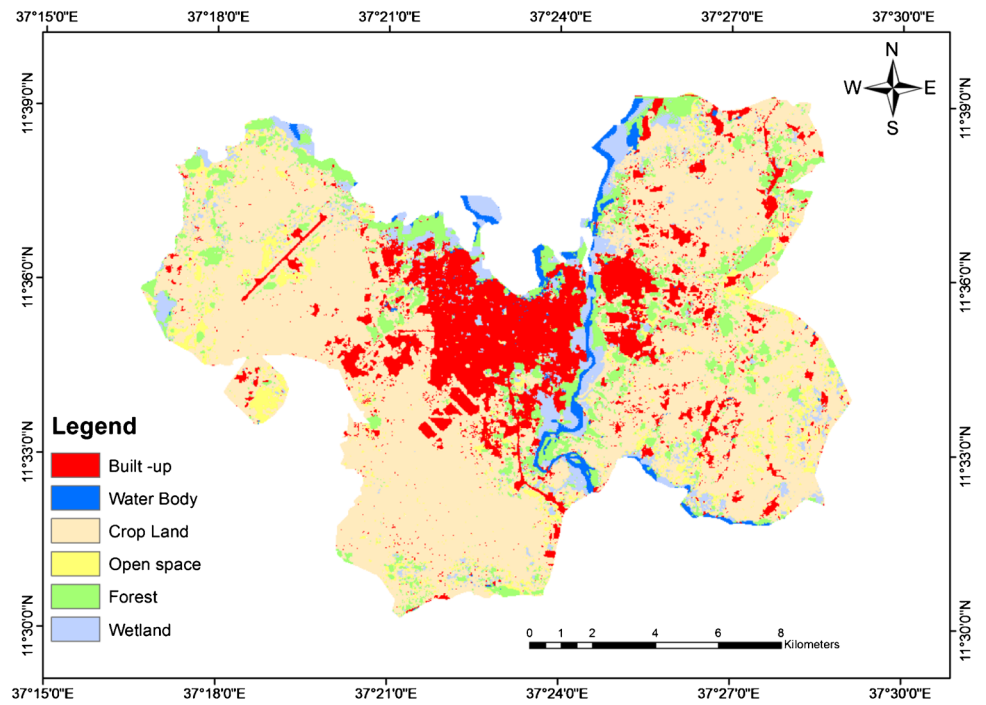


Table 14 Projected LULC of Bahir Dar for 2029, 2039, and 2049

	2029		2039		2049	
	Area (ha)	%	Area (ha)	%	Area (ha)	%
Wetland	1159	5.42	1111	5.15	1350	6.32
Forest	638	2.98	621	2.90	588	2.74
Open space	1460	6.83	1475	6.90	1252	5.86
Crop land	13,787	64.56	13,526	63.33	12,736	59.63
Water body	378	1.77	408	1.91	431	2.01
Built-up	3983	18.61	4214	19.67	4998	23.35

Table 15 Kappa index of agreement to ability to specify quantity and location accurately to predict 2019 LULC map

K indicators	Values
K_{no}	0.8816
$K_{location}$	0.8899
$K_{locationstrata}$	0.8799
$K_{standard}$	0.8483

Table 16 Area of projected and actual land use for 2019

Land use	Actual (2019)		Simulated (2019)		Differences ha
	Area (ha)	%	Area (ha)	%	
Built-up	2566	11.52	2643	12.13	77
Wetland	1767	7.92	1712	7.85	55
Crop land	14,470	64.94	13,963	64.09	507
Open space	1503	6.74	1537	7.05	34
Forest	1620	7.27	1639	7.77	19
Water body	361	1.62	291	1.33	70

that the CA-Markov chain simulation was well designed and that the accuracy assessment was sufficiently accurate.

The total area for the actual LULC map of 2019 was 21,734 ha and the total area for predicted 2019 from the model is 21,319 ha (Table 16). This result shows the model is valid as the overall error is 1.89%, which is negligible. This is calculated by subtracting the total area of the predicted map 2019 from the total area of the actual map of 2019. This result is then converted to a percentage to determine the overall error of the CA-Markov model applied in this study.

Discussion

This report investigated urban growth dynamics and LULC changes over six time periods, 1984–1994, 1994–2009, 2009–2019, 2019–2029, 2029–2039, and 2039–2049. The results presented in the previous section are of interest not only for Bahir Dar City, Ethiopia but also for a more thoughtful reflection on the future urban growth impacts

on the global climate and livelihood of the people and potential factors of urban growth and LULC changes. According to the findings, built-up areas increased by 89.33% between 1984 and 2019, so 2041.1 ha of land has been transformed into artificial surfaces/built-up land during this time. This indicates that urban areas have grown rapidly during the past three and a half decades. Similar studies by Sun et al. (2020) from 2000 to 2017 revealed a high urban growth rate in China's Yangtze River. Their research shows that an increase in the built-up area, combined with rapid urban growth from the core to the periphery, has resulted in a loss of natural land. The present study shows that forest and crop land were decreased while built-up increased due to high scaled and rapid urban growth in the study period. For instance, forest and crop land lost 574.56 ha and 2384.9 ha of its cover from 1984 to 2019. In the same study period, built-up areas showed an increment in its area coverage, i.e., gaining 2286.04 ha, at the expense of the natural land. A study conducted by Martellozzo et al. (2018) on the impact of urban growth on agriculture and natural land indicated that built-up expansion adversely affects the economy and ecology of Italy. Another study (Huang et al. 2020) conducted on the occupation of crop land on global urban growth investigated that the urban occupied 159,170 km² of cropland, accounting for 45.9% of the total expanded urban area, and exerted a significant impact on crop land and its productivity. Such deterioration and natural and semi-natural land loss have become a major worry that practically affects Africa's entire continent (Terfa et al. 2017 and Lasisi et al. 2017), Europe, and Asia.

The findings of this study indicated that crop land had lost a greater percentage of its area than forests between 1984 and 2019. Table 5 reveals that crop land has lost 11.71% of its covers, whereas forests have lost only 2.69% during the same time period. These findings indicated that crop lands are highly vulnerable land use classes strongly affected by rapid urban expansion in Ethiopia. Crop land in the study has been diminishing, and earlier research has cautioned that the loss of crop land and forest might have a significant impact on food security and ecosystem services (Keith et al. 2019; Patra et al. 2018; Wang et al. 2020; Trinder and Liu 2020;

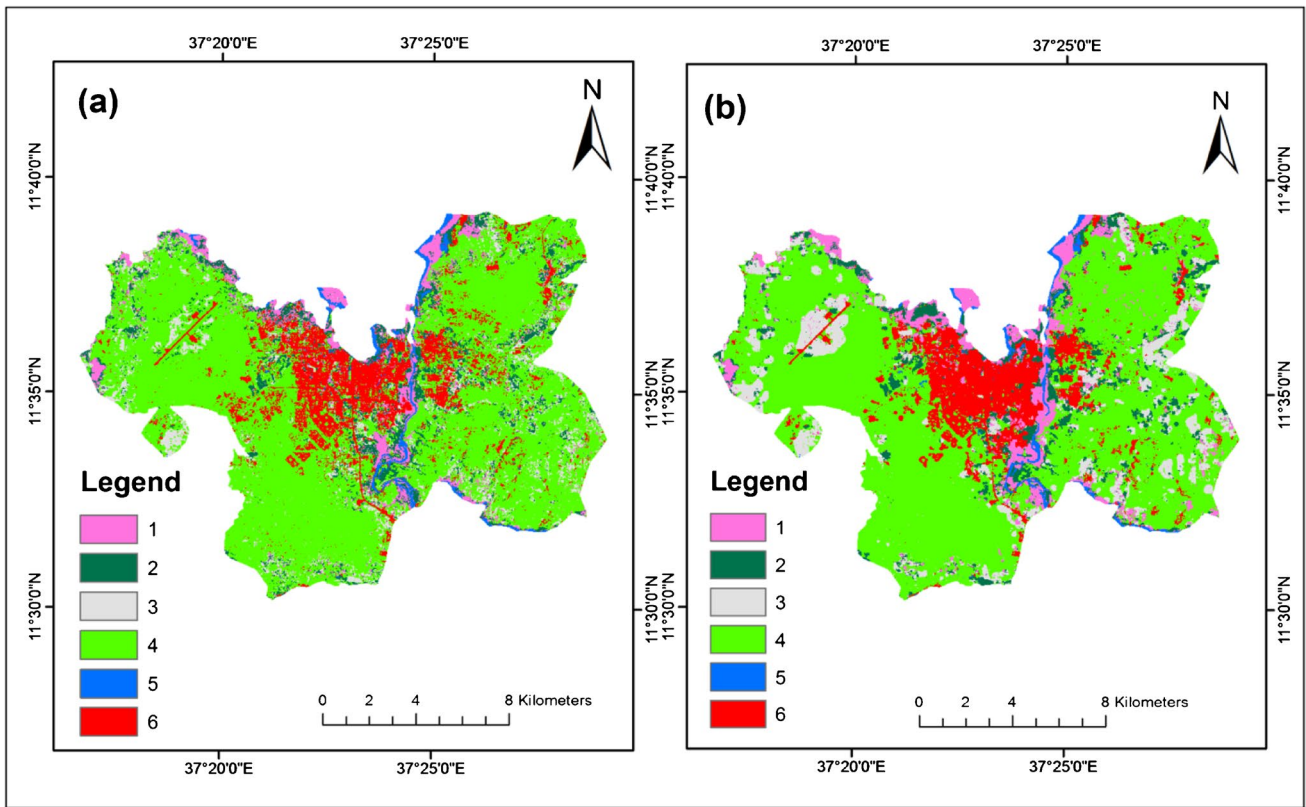
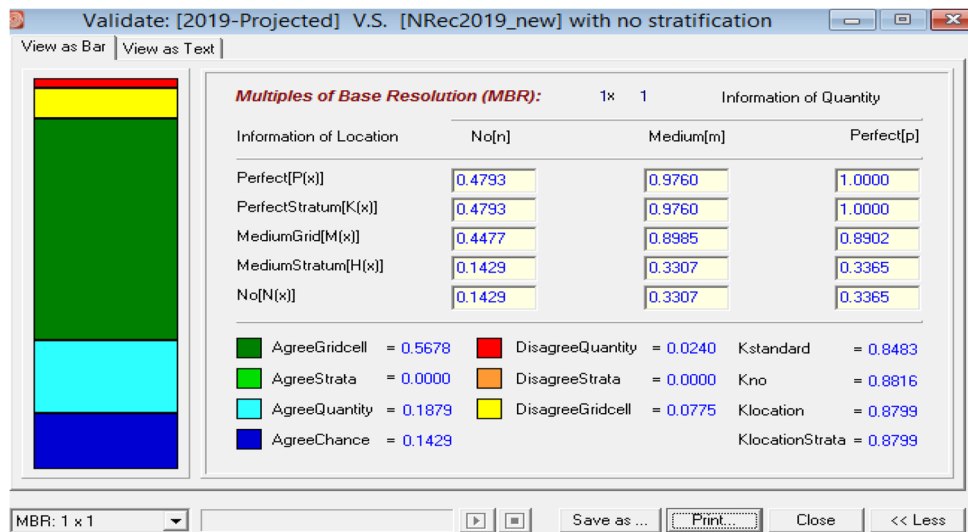


Fig. 9 Actual (a) and projected (b) land cover maps of 2019

Fig. 10 Validation of the model using actual and projected 2019



Basawaraja et al. 2011; Bolca et al. 2007 and Fazal 2000). Previous studies on urban expansion reported that agricultural land is diminishing because of the rapid horizontal expansion and growth of cities and towns in Ethiopia (Alemineh 2018; Ayele and Tarekgn 2020). Research by Asempah et al. (2021) reported that settlement expands eight times the area covered by settlements between 1990 and 2020, i.e., 7.5

km² (1.28%) of land covered by settlement was increased by 59.89 km² (10.33%) in 2020 Wa municipality, Ghana. A similar study conducted in Selangor, Malaysia showed that built-up cover was increased by 608.8 km², whereas natural vegetation was decreased by 831.8 km² from 1999 to 2017 (Azari et al. 2022). Though urban forests can provide necessary ecosystem services to the urban landscape, no study

has reported the positive correlation of urban growth on forest coverage or urban green areas. This indicated that rapid urban growth and land use change have greatly influenced the urban ecology throughout the world (Zhu et al. 2019; Das and Das 2019; Shao et al. 2021). Urban areas in Africa are growing in population and land cover, posing a threat to the continent's ecosystems, biodiversity, and forest coverage. However, the concern over biodiversity and forest land conservation, exacerbated by the expanding urbanization, is overshadowed by the ever-worsening social problems (Seto et al. 2017; Toit et al. 2018). According to studies (Deribew 2020 and Dessu et al. 2020), recent urban expansion and infrastructure development, along with a steep reduction in green space/vegetation, have intensified the intensity and rate of urban growth's impact on the ecosystem and the local climate in the western fringe of Addis Ababa and southwest Ethiopia, respectively.

This study helps to achieve sustainable development goals (SDGs) such as sustainable cities and communities and climate action set by the UN (UN 2018). Rapid urban growth and LULC changes have been affecting the sustainable development of Bahir Dar due to the decline in the forest, wetlands, and open spaces. The growing population has high demand for sanitation, health care, housing, and electricity. Developing countries like Ethiopia cannot afford the cost of these infrastructures and provide basic services to the people, so people are forced to use other options such as clearing green lands and forests to satisfy their demand and basic needs (Asoka et al 2013; Pupilampu and Boafo 2021).

Furthermore, the UN also set another goal of sustainable development called climate action (UN 2018). However, the rapid urban growth and land use transformation in Bahir Dar affect the effort to take urgent action to combat climate change and its impact. Urban growth and rapid land use transformation in Bhir Dar are directly linked to the expansion of manufacturing industry decline in forest and open spaces. This has contributed significantly to increasing greenhouse gases and atmospheric temperature, which are directly linked to climate change (Y. Wang et al. 2014; Mursheed and Yusuf 2018; Milesi and Churkina 2020), so this study helps planners and decision-makers to have detailed information on the current and future urban growth trends and LULC changes in Bahir Dar and develop an appropriate plan and policy to achieve sustainable development in the future.

This study used CA-based Markov chain models to simulate the future urban growth patterns and LULC changes in Bahir Dar city and its surroundings. Various studies were carried out on simulation of urban growth and LULC change in different parts of the world using this model (Shafizadeh and Helbich 2013; Al-sharif and Pradhan 2014; Abutaleb and Ahmed 2016; Altuwajiri et al. 2019; Cai and Wang 2020; Aburas et al. 2021) with different findings. The results obtained from this model indicated that built-up patches will expand in size by 2029, 2039, and 2049. A total of 934 ha is expected to be added to the built-up areas in this time period (coming 30 years). However, in the same time span (2019–2049), crop land and wetland will lose 1736 and 417 ha, respectively (Table 17). This means that built-up areas in the suburbs will expand to the wetlands and crop lands and these land covers will be transformed rapidly into built-up areas (Table 16 and Figs. 6, 7, 8). A study conducted by Mozaffaree and Oja (2021) on urban growth simulated by integrated cellular automata and agent-based models in Tallinn, Estonia reported that the overall built-up areas will reach 175.24 km² with an increase of 30.25% in total from 1990 to 2030. This growth of urban surface would be at the expense of other land uses such as forest and croplands, affecting the urban ecology and agricultural productivity of the community in the urban fringes. Siddiqui et al. (2018) carried out a similar study on urban growth dynamics using CA-MC models and logistic regression in Uttar Pradesh, India, indicating that the city is expected to grow manifolds from 53.6 km² in 1993 to 441.2 km² in 2023. Studies were also conducted by Jat et al. (2017) and Saadani et al. (2020) on urban growth modeling using CA-MC models. The former research revealed that the built-up area is expected to grow manifolds and is expected to have spontaneous growth of urban pixels with a 70% of probability of getting developed in the upcoming years (2015–2040) in Ajmer City of Rajasthan, India. The latter study indicated that built-up area will increase from 29.9 to 43.8 from 2018 to 2040 in EL Jadida City, Moroccan metropolitan due to rapid urban growth and LULC changes. All these studies indicated that urban growth and land use transformation would continue developing in the coming years at the expense of crop land natural lands. Generally, CA–Markov model results revealed that croplands and forests are expected to decline in the upcoming 30 years. In 2049, these two land cover classes will cover 62.37% of the study area, a decrease of 10.48%

Table 17 Quantity of land cover classes in hectares from 2019 to 2049

	Built-up	Wetland	Crop land	Open space	Forest	Water
2019	2566	1767	14,470	1503	1620	361
2029	3938	1159	13,787	1460	638	378
2039	4214	1111	13,526	1475	621	407
2049	4998	1350	12,734	1252	588	431

from the current distribution. This indicates that there will be a significant level of agricultural land and forest loss and land fragmentation in the study area in the upcoming 30 years (Table 16). The present study has validated using kappa statistics such as K_{no} , $K_{location}$, $K_{locationstrata}$, and $K_{standard}$. The K index values are greater than 80%, indicating the presence of strong agreement between the actual and simulated urban growth maps.

The potential factors identified by this study for rapid urban growth and LULC changes in Bahir Dar and its environs are distance from road, slope, distance from CBD, and distance from built-up with its respective weights of 0.29, 0.21, 0.15, and 0.10, respectively. Previous research identified numerous driving factors of urban growth and LULC changes such as physical, proximity, and socio-economic factors (Falah et al. 2020; Hassan and Elhassan 2020; Rana and Sarkar 2021; Liu et al. 2021). For instance, Falah et al. (2020) identified distance from roads, land prices, distance from faults, and distance from the river are the main driving factors of urban growth in Qazvin City. The other study by Mohammadi et al. (2013) reported that distance from highways, roads, residential areas, distance from urban infrastructures, and distance from educational land use were the main factors of urban growth in Isfahan. A similar study shows elevation, slope, soil texture, population density, and distance to commercial area are the main driving factors of urban growth and LULC change (Aburas et al. 2017). These findings indicated that the factors of urban growth and land use change vary over space and time.

Despite the fact that the model employed in this study did an excellent job of simulating the future, there are many uncertainties in the projection of land use classes (Naghbi et al. 2016; Otgonbayar et al. 2018; Li et al. 2020; Chen 2022), which are explained below. First and foremost, it is crucial to notice that the maps which were compared to each other and the actual and projected maps for 2019 differ somehow. Secondly, while the study found that the procedures utilized in the Markov chain model analysis are effective approaches for computing land cover transition probabilities, the procedures were designed with the assumption that transition probabilities do not alter over time (Mozaffaree and Oja 2021). Because the models cannot assess and analyze the changes and processes occurring every time on the landscape structure and LU classes, this causes uncertainty (Memarian et al. 2012). The result, for example, indicates that the transition probabilities from various land covers to wetland and water bodies are high from 1984 to 2019, and the future land changes are modeled using these transition probabilities. However, based on the current distribution, these land covers are expected to decrease dramatically in the years ahead. Lastly, due to unpredictable events such as natural hazards, policy changes, climate changes, and potential uncertainties related to simulator models,

simulation of future LULC would be full of uncertainties (Prestele et al. 2016; Ferchichi et al. 2017). The other limitation of CA-based MC model is its contestant-driven feature rather than a preference-led model, so it lacks dimension of human decision to determine the spatiotemporal dynamics of urban growth in the coming years (Mozaffaree and Oja 2021).

This research reveals that integrating GIS and RS with CA–Markov models provides an enhanced understanding of the futures that Bahir Dar’s terrain will encounter. Facing declining crop, forest, and wetland problems, the projected land use maps will be used as an early warning system to predict and understand the future consequences of urban growth, socio-economic and environmental impacts, and rapid transformation of land use classes to artificial intelligence surfaces. Overall, these findings could be used as a road map/strategic plan for urban planning, assisting urban municipalities/local governments in properly understanding the complex landscape structure and developing improved land use policies and balancing urban growth trends with urban environmental conservations allowing for long-term urban development. CA–Markov modeling should be empirically repeated and further comparative research is needed in the future to evaluate whether these projected landscape changes are specific to Bahir Dar City.

Conclusion

This study demonstrates dynamic simulation of urban growth and land use change using integrated cellular automata and markov chain models: a case of Bahir Dar city, Ethiopia, to detect changes in the area by comparing images between 2 years. Based on the CA–Markov models, the probability of changes in Bahir Dar City and its surroundings was predicted. Built-up (urban) area increased from 243.94 to 2529.98 ha, whereas crop land was decreased by 11.17% from 1984 to 2019. Results predicted by CA–Markov model indicate that over the upcoming years, the city’s rapid expansion into its environs, particularly on the western and eastern fronts, will be more intense and faster than on the other fronts. Based on the results of this study, cropland will decrease from 137.87 km² in 2029 to 135.26 km² in 2039 and 135.56 km² in 2039 to 127.36 km² in 2049 km². However, a continuous increase in built-up area will be observed in 2029 39.38 km² (18.61%), 2039 42.14 km² (19.69%), and 2049 49.98 km² (23.35%). Distance from road, slope, CBD, distance from built-up, and distance from airport are the most effective driving factors of urban growth in Bahir Dar with a final weight of 0.29, 0.21, 0.15, 0.10, and 0.076 respectively.

Forests and crop lands will primarily transit to urban artificial surfaces as built-up areas expand and eventually

promote rapid urbanization and unplanned settlements. These gains in urban patches will result from losses in crop land and forests in 2029, 2039, and 2049, which will cause a reduction in soil productivity and increase flooding. These gradual changes will result in social and economic marginalization, mainly in eastern and western fringes. Therefore, sustainable development of Bahir Dar can be achieved if high priority is given to urban growth management by planners and decision-makers. The CA-based model has the ability to represent non-linear, spatial, and stochastic processes.

Furthermore, the CA-based MC model can model and control complex spatially distributed processes and provide clear insights into local behaviors and global land use/cover change patterns. Moreover, spatial and temporal complexities of land use change can be well represented and simulated using suitable transition rules in CA model. CA–Markov model also has some disadvantages; it cannot handle the top-down processes. The study was conducted based on medium resolution (30 m) satellite images, so this could affect the results related to LULC maps because multiple land use land cover classes were prevalent in single pixels. For instance, water bodies could not be mapped due to the coarser resolution of satellite images. The other limitation of this study is lack of required data related to population density. Population density map is necessary for this study, but due to lack of this necessary data, the variable is excluded from the list of driving factors of urban growth and land use changes. The mapping of urban growth using GIS and RS as well as urban growth and LULC change modeling using CA–Markov models could have significant contribution for future urban growth management in Bahir Dar and can be an instrument for a decision support system for urban planners and policy makers to design urban growth plans with an approach of sustainable habitat development. This study recommends the application of integrated simulation models of CA–Markov and agent-based model (ABM) for the same study area and draw comparisons of results obtained from both models to overcome the CA–Markov barriers for future work.

Declarations

Conflict of interest The authors declare no competing interests.

References

- Aburas MM, Ho YM, Ramli MF, Ash'aari ZH (2017) Improving the capability of an integrated CA–Markov model to simulate spatio-temporal urban growth trends using an analytical hierarchy process and frequency ratio. *Int J Appl Earth Obs Geoinf* 59:65–78. <https://doi.org/10.1016/j.jag.2017.03.006>
- Aburas MM, Ho YM, Pradhan B, Salleh AH, Alazaiza MY (2021) Spatio-temporal simulation of future urban growth trends using an integrated CA–Markov model. *Arab J Geosci* 14(2):131. <https://doi.org/10.1007/s12517-021-06487-8>
- Abutaleb K, Ahmed F (2016) Modeling of urban change using remote sensing data and cellular automata technique. *Arab J Geosci* 9(15):1–10. <https://doi.org/10.1007/s12517-016-2696-z>
- Aithal BH, Ramachandra TV (2016) Visualization of urban growth pattern in Chennai using geoinformatics and spatial metrics. *J Indian Soc Remote Sens* 44(4):617–633. <https://doi.org/10.1007/s12524-015-0482-0>
- Akintunde JA (2019) Spatial pattern of urban growth using remote sensing and landscape metrics. *J Geomat* 13(1):53–60
- Al-sharif AA, Pradhan B (2014) Monitoring and predicting land use change in Tripoli Metropolitan City using an integrated Markov chain and cellular automata models in GIS. *Arab J Geosci* 7(10):4291–4301. <https://doi.org/10.1007/s12517-013-1119-7>
- Alaei MS, Karimi M, Habibi K (2020) Modelling urban growth incorporating spatial interactions between the cities: the example of the Tehran metropolitan region. *Environ Plan B Urban Anal City Sci* 47(6):1047–1064. <https://doi.org/10.1177/239980831816701>
- Alemineh YT (2018) Livelihood changes, and related effects of urban expansion on urban peripheral communities : the case of Gondar City : ANRS. *J Poverty Invest Dev* 45:50–56. ISSN 2422–846X
- Alemu ZG, Oosthuizen K, Van SH (2003) Contribution of agriculture in the Ethiopian economy: a time-varying parameter approach. *Agrekon* 42(1):29–48. <https://doi.org/10.1080/03031853.2003.9523608>
- Alsharif AAA, Pradhan B (2014) Urban sprawl analysis of Tripoli Metropolitan City (Libya) using remote sensing data and multivariate logistic regression model. *J Indian Soc Remote Sens* 42(1):149–163. <https://doi.org/10.1007/s12524-013-0299-7>
- Altuwajri HA, Alotaibi MH, Almudlaj AM, Almalki FM (2019) Predicting urban growth of Arriyadh city, capital of the Kingdom of Saudi Arabia, using Markov cellular automata in TerrSet geospatial system. *Arab J Geosci* 12(4):1–15. <https://doi.org/10.1007/s12517-019-4261-z>
- Appelhans N (2017) Urban planning and everyday urbanisation: a case study on Bahir Dar, Ethiopia. <https://doi.org/10.14361/9783839437155>
- Arsanjani JJ, Helbich M, Kainz W, Boloorani AD (2012) Integration of logistic regression, Markov chain and cellular automata models to simulate urban expansion. *Int J Appl Earth Obs Geoinf* 21(1):265–275. <https://doi.org/10.1016/j.jag.2011.12.014>
- Assefa WW, Eneyew BG, Wondie A (2021) The impacts of land-use and land-cover change on wetland ecosystem service values in peri-urban and urban area of Bahir Dar City, Upper Blue Nile Basin, Northwestern Ethiopia. *Ecol Process* 10(1):1–18. <https://doi.org/10.1186/s13717-021-00310-8>
- Aswal P, Saini R, Tanzeem M (2018) Spatio temporal monitoring of urban sprawl using GIS and remote sensing technique. *Int J Comput Appl* 182(27):11–24. <https://doi.org/10.5120/ijca2018918100>
- Asempah M, Sahwan W, Schütt B (2021) Assessment of land cover dynamics and drivers of urban expansion using geospatial and logistic regression approach in Wa municipality, Ghana. *Land* 10(11):1251. <https://doi.org/10.3390/land10111251>
- Asoka GW, Thuo AD, Bunyasi MM (2013) Effects of population growth on urban infrastructure and services: a case of Eastleigh neighborhood Nairobi, Kenya. *J Anthropol Archaeol* 1(1):41–56. Retrieved from www.aripd.org/jaa
- Ayele A, Tarekegn K (2020) The impact of urbanization expansion on agricultural land in Ethiopia: a review. *Environ Socio-Econ Stud* 8(4):73–80. <https://doi.org/10.2478/enviro-2020-0024>
- Azari M, Billa L, Chan A (2022) Multi-temporal analysis of past and future land cover change in the highly urbanized state of Selangor, Malaysia. *Ecol Process* 11(2). <https://doi.org/10.1186/s13717-021-00350-0>

- Basawaraja R, Chari KB, Mise SR, Chetti SB (2011) Analysis of the impact of urban sprawl in altering the land-use, land-cover pattern of Raichur City, India, using geospatial technologies. *J Geogr Reg Plann* 4(8):455–462. <http://www.academicjournals.org/JGRP>
- Berila A, Isufi F (2021) Two Decades (2000–2020) Measuring urban sprawl using GIS, RS and landscape metrics: a case study of municipality of Prishtina (Kosovo). *J Ecol Eng* 22(6):114–115. <https://doi.org/10.12911/22998993/137070>
- Blecic I, Cecchini A, Prastacos P, Trunfio GA, Verigos E (2004) Modeling urban dynamics with cellular automata: a model of the city of Heraclion. 7th AGILE Conference on Geographic Information Science, University of Crete Press, Heraklion, Greece 313–323. http://agile.gis.geo.tu-dresden.de/Conference_Paper/CDs/agile_2004/papers/4-1-2_Blecic.pdf
- Bolca M, Turkyilmaz B, Kurucu Y, Altinbas U, Esetlili MT, Gulgun B (2007) Determination of impact of urbanization on agricultural land and wetland land use in Balçova's Delta by remote sensing and GIS technique. *Environ Monit Assess* 131(1–3):409–419. <https://doi.org/10.1007/s10661-006-9486-0>
- Cai L, Wang M (2020) Effect of the thematic resolution of land use data on urban expansion simulations using the CA-Markov model. *Arab J Geosci* 13(23):1250. <https://doi.org/10.1007/s12517-020-06248-z>
- Chen Y (2022) An extended patch-based cellular automaton to simulate horizontal and vertical urban growth under the shared socioeconomic pathways. *Comput Environ Urban Syst* 91:101727. <https://doi.org/10.1016/j.compenvurbsys.2021.101727>
- Congalton RG (2001) Accuracy assessment and validation of remotely sensed and other spatial information. *Int J Wildland Fire* 10(3–4):321–328. <https://doi.org/10.1071/wf01031>
- Cui N, Feng C, Han R, Guo L (2019) Impact of urbanization on ecosystem health : a case study in Zhuhai, China. *Int J Environ Res Public Health* 16(23):4717. <https://www.mdpi.com/1660-4601/16/23/4717#>
- Das M, Das A (2019) Dynamics of urbanization and its impact on urban ecosystem services (UESs): a study of a medium size town of West Bengal, Eastern India. *J Urban Manag* 8(3):420–434. <https://doi.org/10.1016/j.jum.2019.03.002>
- Almeida CM, Batty M, Monteiro AM, Câmara G, Filho BS, Cerqueira GC, Pennachin CL (2003) Stochastic cellular automata modeling of urban land use dynamics: empirical development and estimation. *Comput Environ Urban Syst* 27(5):481–509. [https://doi.org/10.1016/S0198-9715\(02\)00042-X](https://doi.org/10.1016/S0198-9715(02)00042-X)
- Deribew KT (2020) Spatiotemporal analysis of urban growth on forest and agricultural land using geospatial techniques and Shannon entropy method in the satellite town of Ethiopia, the western fringe of Addis Ababa city. *Ecol Process* 9(1). <https://doi.org/10.1186/s13717-020-00248-3>
- Dessu T, Korecha D, Hunde D, Worku A (2020) Long-term land use land cover change in urban centers of Southwest Ethiopia from a climate change perspective. *Front Clim* 2(577168):1–23. <https://doi.org/10.3389/fclim.2020.577169>
- Falah N, Karimi A, Harandi AT (2020) Urban growth modeling using cellular automata model and AHP (case study: Qazvin city). *Model Earth Syst Environ* 6(1):235–248. <https://doi.org/10.1007/s40808-019-00674-z>
- Fan F, Wang Y, Wang Z (2008) Temporal and spatial change detecting (1998–2003) and predicting of land use and land cover in Core corridor of Pearl River Delta (China) by using TM and ETM+ images. *Environ Monit Assess* 137(1–3):127–147. <https://doi.org/10.1007/s10661-007-9734-y>
- Fazal S (2000) Urban expansion and loss of agricultural land - a GIS based study of Saharanpur City, India. *Environ Urban* 12(2):133–149. <https://doi.org/10.1177/095624780001200211>
- Ferchichi A, Boulila W, Farah IR (2017) Towards an uncertainty reduction framework for land-cover change prediction using possibility theory. *Vietnam J Comput Sci* 4(3):195–209. <https://doi.org/10.1007/s40595-016-0088-7>
- Fitawok MB, Derudder B, Minale AS, Passel SV, Adgo E, Nyssen J (2020) Modeling the impact of urbanization on land-use change in Bahir Dar City, Ethiopia: an integrated cellular automata-Markov chain approach. *Land* 9(4):1–17. <https://doi.org/10.3390/land9040115>
- Gómez JA, Patiño JE, Duque JC, Passos S (2020) Spatiotemporal modeling of urban growth using machine learning. *Remote Sens* 12(1). <https://doi.org/10.3390/rs12010109>
- Goncalves TM, Zhong X, Ziggah YY, Dwamena BY (2019) Simulating urban growth using cellular automata approach (SLEUTH)-a case study of Praia City, Cabo Verde. *IEEE Access* 7:156430–156442. <https://doi.org/10.1109/ACCESS.2019.2949689>
- Guangjin T, Xinliang X, Xiaojuan L, Lingqiang K (2016) The comparison and modeling of the driving factors of urban expansion for thirty-five big cities in the three regions in China. *Adv Meteorol*. <https://doi.org/10.1155/2016/3109396>
- Habibi S, Asadi N (2011) Causes, results and methods of controlling urban sprawl. *Procedia Eng* 21:133–141. <https://doi.org/10.1016/j.proeng.2011.11.1996>
- Halmy MW, Gessler PE, Hicke JA, Salem BB (2015) Land use/land cover change detection and prediction in the north-western coastal desert of Egypt using Markov-CA. *Appl Geogr* 63:101–112. <https://doi.org/10.1016/j.apgeog.2015.06.015>
- Hamdy O, Zhao S, Osman T, Salheen MA, Eid YY (2016) Applying a hybrid model of markov chain and logistic regression to identify future urban sprawl in Abouelreesh, Aswan: a case study. *Geosci* 6(4):3. <https://doi.org/10.3390/geosci6040043>
- Hamdy O, Zhao S, Salheen MA, Eid YY (2017) Analyses the driving forces for urban growth by using IDRISI @ Selva models Abouelreesh Aswan as a case study. *Int J Eng Technol* 9(3). <https://doi.org/10.7763/IJET.2017.V9.975>
- Hassan MI, Elhassan SM (2020) Modelling of Urban Growth and Planning: A Critical Review. *J Build Constr Plan Res* 08(04):245–262. <https://doi.org/10.4236/jbcrp.2020.84016>
- Hasan S, Shi W, Zhu X (2020) Impact of land use land cover changes on ecosystem service value - a case study of Guangdong, Hong Kong, and Macao in South China. *PLoS ONE* 15(4):1–20. <https://doi.org/10.1371/journal.pone.0231259>
- Hassan Z, Shabbir R, Ahmad SS, Malik AH, Aziz N, Butt A, Erum S (2016) Dynamics of land use and land cover change (LULCC) using geospatial techniques: a case study of Islamabad Pakistan. *SpringerPlus* 5(1). <https://doi.org/10.1186/s40064-016-2414-z>
- Helbich M, Leitner M (2009) Spatial analysis of the urban-to-rural migration determinants in the Viennese metropolitan area. A transition from suburbia to postsuburbia? *Appl Spat Anal Policy* 2(3):237–260. <https://doi.org/10.1007/s12061-009-9026-8>
- Hisham S, Jarah A, Zhou B, Abdullah RJ, Lu Y, Yu W (2019) Urbanization and urban sprawl issues in city structure: a case of the Sulaymaniah Iraqi Kurdistan region. *Sustainability* 11(2):485. <https://doi.org/10.3390/su11020485>
- Huang Q, Liu Z, He C, Gou S, Bai Y, Wang Y, Shen M (2020) The occupation of cropland by global urban expansion from 1992 to 2016 and its implications. *Environ Res Lett* 15(8). <https://doi.org/10.1088/1748-9326/ab858c>
- Ismail MH (2009) Evaluating supervised and unsupervised techniques for land cover mapping using remote sensing data. *Geografia Malays J Soc Space* 5(1):1–10. ISSN 2180–2491
- Jafari M, Majedi H, Monavari SM, Alesheikh AA, Zarkesh MK (2016) Dynamic simulation of urban expansion through a CA-markov model case study: Hyrcanian region, Gilan, Iran. *Eur J Remote Sens* 49:513–529. <https://doi.org/10.5721/EuJRS20164927>

- Jat MK, Choudhary M, Saxena A (2017) Application of geospatial techniques and cellular automata for modelling urban growth of a heterogeneous urban fringe. *Egypt J Remote Sens Space Sci* 20(2):223–241. <https://doi.org/10.1016/j.ejrs.2017.02.002>
- Kasraian D, Maat K, Van WB (2019) The impact of urban proximity, transport accessibility and policy on urban growth: a longitudinal analysis over five decades. *Environ Plan B Urban Anal City Sci* 46(6):1000–1017. <https://doi.org/10.1177/2399808317740355>
- Keith C, Lyu R, Zhang J, Xu M, Li J (2019) Impacts of urbanization on ecosystem services and their temporal relations: a case study in Northern Ningxia, China. *Land Use Policy* 77:163–173. <https://doi.org/10.1016/j.compenvurbsys.2019.101351>
- Keshkar H, Voigt W (2016) A spatiotemporal analysis of landscape change using an integrated Markov chain and cellular automata models. *Model Earth Syst Environ* 2(1):1–13. <https://doi.org/10.1007/s40808-015-0068-4>
- Kharel G (2010) Impacts of urbanization on environmental resources: a land use planning perspective. MSc. Thesis, The University of Texas at Arlington
- Lasisi M, Popoola A, Adediji A, Adedeji O, Babalola K (2017) City expansion and agricultural land loss within the peri-urban area of Osun State, Nigeria. *Ghana J Geogr* 9(3):132–163. ISSN: 0855–9414
- Lawal DU, Matori AN, Balogun AL (2011) A geographic information system and multi-criteria decision analysis in proposing new recreational park sites in Universiti Teknologi Malaysia. *Mod Appl Sci* 5(3):39–55. <https://doi.org/10.5539/mas.v5n3p39>
- Li M, Zang S, Zhang B, Li S, Wu C (2014) A review of remote sensing image classification techniques: the role of spatio-contextual information. *Eur J Remote Sens* 47(1):389–411. <https://doi.org/10.5721/EuJRS20144723>
- Li G, Sun S, Fang C (2018) The varying driving forces of urban expansion in China: insights from a spatial-temporal analysis. *Landsc Urban Plan* 174:63–77. <https://doi.org/10.1016/j.landurbplan.2018.03.004>
- Li M, Zhang G, Liu Y, Cao Y, Zhou C (2019) Determinants of urban expansion and spatial heterogeneity in China. *Int J Environ Res Public Health* 16(19):3706. <https://doi.org/10.3390/ijerph16193706>
- Li X, Zhou Y, Chen W (2020) An improved urban cellular automata model by using the trend-adjusted neighborhood. *Ecol Process* 9(1). <https://doi.org/10.1186/s13717-020-00234-9>
- Liao C, Dai T, Cai H, Zhang W (2017) Examining the driving factors causing rapid urban expansion in China: an analysis based on GlobeLand30 data. *ISPRS International Journal of Geo-Inf* 6(9):264. <https://doi.org/10.3390/ijgi6090264>
- Lindström J, Eklundh L, Holst J, Holst U (2006) Influence of solar zenith angles on observed trends in the NOAA/NASA 8-km Pathfinder normalized difference vegetation index over the African Sahel. *Int J Remote Sens* 27(10):1973–1991. <https://doi.org/10.1080/01431160500380539>
- Liping C, Yujun S, Saeed S (2018) Monitoring and predicting land use and land cover changes using remote sensing and GIS techniques—a case study of a hilly area, Jiangle, China. *Plos ONE* 13(7):1–23. <https://doi.org/10.1371/journal.pone.0200493>
- Lity P (2021) Macroeconomic perspective on urban sprawl : a multi-dimensional approach in Poland. *Land* 10(116). <https://doi.org/10.3390/land10020116>
- Liu Y, He J (2009) Developing a web-based cellular automata model for urban growth simulation. *International Symposium on Spatial Analysis, Spatial-Temporal Data Modeling, and Data Mining* 7492:74925C. <https://doi.org/10.1117/12.838657>
- Liu Y, Batty M, Wang S, Corcoran J (2021) Modelling urban change with cellular automata: contemporary issues and future research directions. *Prog Hum Geogr* 45(1):3–24. <https://doi.org/10.1177/0309132519895305>
- Maithani S (2010a) Application of cellular automata and GIS techniques in urban growth modelling: a new perspective. *Inst Town Plan India J* 7–1(1):36–49
- Maithani S (2010b) Cellular automata based model of urban spatial growth. *J Indian Soc Remote Sens* 38(4):604–610. <https://doi.org/10.1007/s12524-010-0053-3>
- Martellozzo F, Amato F, Murgante B, Clarke KC (2018) Modelling the impact of urban growth on agriculture and natural land in Italy to 2030. *Appl Geogr* 91:156–167. <https://doi.org/10.1016/j.apgeog.2017.12.004>
- Mehriar M, Masoumi H, Mohino I (2020) Urban sprawl, socio-economic features, and travel patterns in middle east countries: a case study in Iran. *Sustainability* 12(22):1–20. <https://doi.org/10.3390/su12229620>
- Memarian H, Balasundram SK, Talib J, Bin TC, Sung B, Sood AM, Abbaspour K (2012) Validation of CA-Markov for simulation of land use and cover change in the Langat Basin, Malaysia. *J Geogr Inf Syst* 4:542–554
- Milesi C, Churkina G (2020) Measuring and monitoring urban impacts on climate change from space. *Remote Sens* 12(21):1–25. <https://doi.org/10.3390/rs12213494>
- Mishra BK, Mebeelo K, Chakraborty S, Kumar P, Gautam A (2021) Implications of urban expansion on land use and land cover: towards sustainable development of Mega Manila, Philippines. *Geojournal* 86(2):927–942. <https://doi.org/10.1007/s10708-019-10105-2>
- Mohammadi M, Sahebgharani A, Malekipour E (2013) Urban growth simulation through cellular automata (CA), analytic hierarchy process (AHP) and GIS; case study of 8th and 12th municipal districts of Isfahan. *Geogr Tech* 08(2):57–70
- Mohammadzadeh MJ, Karbassi AR, Nabi BG, Abbaspour M (2016) Integrated environmental management model of air pollution control by hybrid model of DPSIR and FAHP. *Glob J Environ Sci Manag* 2(4):381–388. <https://doi.org/10.22034/gjesm.2016.02.04.007>
- Mosammam HM, Nia JT, Khani H, Teymouri A, Kazemi M, Mohammadian H, Khani H (2017) Monitoring land use change and measuring urban sprawl based on its spatial forms: the case of Qom city. *Egypt J Remote Sens Space Sci* 20(1):103–116. <https://doi.org/10.1016/j.ejrs.2016.08.002>
- Mozaffaree PN, Oja T (2021) Urban expansion simulated by integrated cellular automata and agent-based models; an example of Tallinn, Estonia. *Urban Sci* 5(4):85. <https://doi.org/10.3390/urbansci5040085>
- Murshed M, Yusuf SS (2018) Effects of urbanization on climate change: evidence from Bangladesh. *Bangladesh view project independent review of Bangladesh's development view project*. *J Nat Sci Res* 8. ISSN 2224–3186
- Myagmartseren P, Ganpurev D, Myagmarjav I, Byambakhuu G, Dabuxile G (2020) Remote sensing and multivariate logistic regression model for the estimation of urban expansion (case of Darkhan City, Mongolia). *Int Arch Photogramm Remote Sens Spat Inf Sci - ISPRS Arch* 43(B3):721–726. <https://doi.org/10.5194/isprs-archives-XLIII-B3-2020-721-2020>
- Naghbi F, Delavar MR, Pijanowski B (2016) Urban growth modeling using cellular automata with multi-temporal remote sensing images calibrated by the artificial bee colony optimization algorithm. *Sensors* 16(12):2122. <https://doi.org/10.3390/s16122122>
- Nguyen T (2015) Optimal ground control points for geometric correction using genetic algorithm with global accuracy. *Eur J Remote Sens* 48:85–99. <https://doi.org/10.5721/EuJRS20154806>
- Omar NQ, Ahamad MS, Wan HW, Samat N, Binti AS (2014) Markov CA, multi regression, and multiple decision making for modeling historical changes in Kirkuk City, Iraq. *J Indian Soc Remote Sens* 42(1):165–178. <https://doi.org/10.1007/s12524-013-0311-2>

- Otgonbayar M, Badarifu RT, Onishi T, Hiramatsu K (2018) Cellular automata modelling approach for urban growth. *Rev Agric Sci* 6:93–104. <https://doi.org/10.7831/ras.6.93>
- Ozdemir MS, Saaty TL (2006) The unknown in decision making. What to do about it. *Eur J Oper Res* 174(1):349–359. <https://doi.org/10.1016/j.ejor.2004.12.017>
- Parsa VA, Salehi E (2016) Spatio-temporal analysis and simulation pattern of land use/cover changes, case study_ Naghadeh, Iran. *J Urban Manag* 5(2):43–51. <https://doi.org/10.1016/j.jum.2016.11.001>
- Patra S, Sahoo S, Mishra P, Mahapatra SC (2018) Impacts of urbanization on land use/cover changes and its probable implications on local climate and groundwater level. *J Urban Manag* 7(2):70–84. <https://doi.org/10.1016/j.jum.2018.04.006>
- Pontius RG (2000) Quantification error versus location error in comparison of categorical maps. *Photogramm Eng Remote Sens* 66(8):1011–1016. 0099–1112/00/6608–1011\$3.00
- Pontius RG, Cornell JD, Hall CA (2001) Modeling the spatial pattern of land-use change with GEOMOD2: application and validation for Costa Rica. *Agric Ecosyst Environ* 85(1–3):191–203. [https://doi.org/10.1016/S0167-8809\(01\)00183-9](https://doi.org/10.1016/S0167-8809(01)00183-9)
- Prestele R, Alexander P, Rounsevell MDA, Arneth A, Calvin K, Doelman J, Verburg PH (2016) Hotspots of uncertainty in land-use and land-cover change projections: a global-scale model comparison. *Glob Change Biol* 22(12):3967–3983. <https://doi.org/10.1111/gcb.13337>
- Puplampu DA, Bofo YA (2021) Exploring the impacts of urban expansion on green spaces availability and delivery of ecosystem services in the Accra metropolis. *Environ Challenges* 5:100283. <https://doi.org/10.1016/j.envc.2021.100283>
- Rana MS, Sarkar S (2021) Prediction of urban expansion by using land cover change detection approach. *Heliyon* 7(11):8437. <https://doi.org/10.1016/j.heliyon.2021.e08437>
- Rawat JS, Kumar M (2015) Monitoring land use/cover change using remote sensing and GIS techniques: a case study of Hawalbagh block, district Almora, Uttarakhand, India. *Egypt J Remote Sens Space Sci* 18(1):77–84. <https://doi.org/10.1016/j.ejrs.2015.02.002>
- Rimal B, Zhang L, Keshtkar H, Wang N, Lin Y (2017) Monitoring and modeling of spatiotemporal urban expansion and land-use/land-cover change using integrated Markov chain cellular automata model. *ISPRS Int J GeoInf* 6(9):1–21. <https://doi.org/10.3390/ijgi6090288>
- Rimal B, Zhang L, Keshtkar H, Haack BN, Rijal S, Zhang P (2018) Land use/land cover dynamics and modeling of urban land expansion by the integration of cellular automata and Markov chain. *ISPRS Int J GeoInf* 7(4):154. <https://doi.org/10.3390/ijgi7040154>
- Saadani S, Laajaj R, Maanan M, Rhinane H, Aaroud A (2020) Simulating spatial–temporal urban growth of a Moroccan metropolitan using CA–Markov model. *Spat Inf Res* 28(5):609–621. <https://doi.org/10.1007/s41324-020-00322-0>
- Saaty RW (1987) The analytic hierarchy process-what it is and how it is used. *Math Model* 9(3–5):161–176. [https://doi.org/10.1016/0270-0255\(87\)90473-8](https://doi.org/10.1016/0270-0255(87)90473-8)
- Salem M, Bose A, Bashir B, Basak D, Roy S, Chowdhury IR, Tsurusaki N (2021) Urban expansion simulation based on various driving factors using a logistic regression model: Delhi as a case study. *Sustainability* 13(19):1–17. <https://doi.org/10.3390/su131910805>
- Samat N (2009) Integrating GIS and CA-Markov model in evaluating urban spatial growth. *Malays J Environ Manag* 10(1):83–100
- Samat N, Hasni R, Elhadary YA (2011) Modelling land use changes at the peri-urban areas using geographic information systems and cellular automata model. *J Sustain Dev* 4(6):72–84. <https://doi.org/10.5539/jsd.v4n6p72>
- Sang L, Zhang C, Yang J, Zhu D, Yun W (2011) Simulation of land use spatial pattern of towns and villages based on CA-Markov model. *Math Comput Model* 54(3–4):938–943. <https://doi.org/10.1016/j.mcm.2010.11.019>
- Santé I, García AM, Miranda D, Crecente R (2010) Cellular automata models for the simulation of real-world urban processes: a review and analysis. *Landsc Urban Plan* 96(2):108–122. <https://doi.org/10.1016/j.landurbplan.2010.03.001>
- Seto KC, Güneralp B, Hutyrá LR (2012) Global forecasts of urban expansion to 2030 and direct impacts on biodiversity and carbon pools. *Proc Natl Acad Sci USA* 109(40):16083–16088. <https://doi.org/10.1073/pnas.1211658109>
- Seto KC, Schneider A, Mertes CM, Mitchell T (2017) Urbanization in Africa: challenges and opportunities for conservation. *Environ Res Lett* 13(1):15002
- Shafizadeh MH, Helbich M (2013) Spatiotemporal urbanization processes in the megacity of Mumbai, India: a Markov chains-cellular automata urban growth model. *Appl Geogr* 40:140–149. <https://doi.org/10.1016/j.apgeog.2013.01.009>
- Shao Z, Sumari NS, Portnov A, Ujoh F, Musakwa W, Mandela PJ (2021) Urban sprawl and its impact on sustainable urban development: a combination of remote sensing and social media data. *Geo-Spat Inf Sci* 24(2):241–255. <https://doi.org/10.1080/10095020.2020.1787800>
- Siddiqui A, Siddiqui A, Maithani S, Jha AK, Kumar P, Srivastav SK (2018) Urban growth dynamics of an Indian metropolitan using CA Markov and Logistic Regression. *Egypt J Remote S Space Sci* 21(3):229–236. <https://doi.org/10.1016/j.ejrs.2017.11.006>
- Silver D, Silva TH (2021) A Markov model of urban evolution: neighbourhood change as a complex process. *PLoS ONE* 16(1):1–29. <https://doi.org/10.1371/journal.pone.0245357>
- Sun W, Shan J, Wang Z, Wang L, Lu D, Jin Z, Yu K (2020) Geospatial analysis of urban expansion using remote sensing methods and data: a case study of Yangtze River Delta, China. *Complexity* 12. <https://doi.org/10.1155/2020/3239471>
- Surya B, Ahmad DN, Sakti HH, Sahban H (2020) Land use change, spatial interaction, and sustainable development in the metropolitan urban areas, south Sulawesi province, Indonesia. *Land* 9(3):95. <https://doi.org/10.3390/land9030095>
- Tajbakhsh M, Memarian H, Shahrokhi Y (2016) Analyzing and modeling urban sprawl and land use changes in a developing city using a CA-Markovian approach. *Glob J Environ Sci Manag* 2(4):397–410. <https://doi.org/10.22034/gjesm.2016.02.04.009>
- Terfa BK, Chen N, Liu D, Zhang X, Niyogi D (2017) Urban expansion in Ethiopia from 1987 to 2017: characteristics, spatial patterns, and driving forces. *Sustainability* 11(10):1–21. <https://doi.org/10.3390/SU11102973>
- Toit MJ, Cilliers SS, Dallimer M, Goddard M, Guenat S, Cornelius SF (2018) Urban green infrastructure and ecosystem services in sub-Saharan Africa. *Landsc Urban Plan* 180:249–261. <https://doi.org/10.1016/j.landurbplan.2018.06.001>
- Torrens PM (2001) Can geocomputation save urban simulation? Throw some agents into the mixture, simmer and wait. *CASA Working Paper* (32). Center for Advanced Spatial Analysis (UCL), London, UK. <http://www.casa.ucl.ac.uk/paper31.pdf> <http://www.geosimulation.com>.
- Triantakostas D, Mountrakis G (2012) Urban growth prediction: a review of computational models and human perceptions. *J Geogr Inf Syst* 04(06):555–587. <https://doi.org/10.4236/jgis.2012.46060>
- Trinder J, Liu Q (2020) Assessing environmental impacts of urban growth using remote sensing. *Geo Spat Inf Sci* 23(1):20–39. <https://doi.org/10.1080/10095020.2019.1710438>
- Tripathy P, Bandopadhyay A (2018) Urban growth modeling using logistic regression and geo-informatics : a case of Jaipur, India. *Soc Environ Dev* 13: 47–62. ISSN: 0975–7120

- Turok I, McGranahan G (2013) Urbanization and economic growth: the arguments and evidence for Africa and Asia. *Environ Urban* 25(2):465–482. <https://doi.org/10.1177/0956247813490908>
- UN (2018) The 2030 agenda and the sustainable development goals An opportunity for Latin America and the Caribbean. (LC/G.2681-P/Rev.3), Santiago
- Wang SQ, Zheng XQ, Zang XB (2012) Accuracy assessments of land use change simulation based on Markov-cellular automata model. *Procedia Environ Sci* 13(2011):1238–1245. <https://doi.org/10.1016/j.proenv.2012.01.117>
- Wang Y, Ji W, Yu X, Xu X, Jiang D, Wang Z, Zhuang D (2014) The impact of urbanization on the annual average temperature of the past 60 years in Beijing. *Adv Meteorol* 1:9. <https://doi.org/10.1155/2014/374987>
- Wang W, Wu T, Li Y, Xie S, Han B, Zheng H, Ouyang Z (2020) Urbanization impacts on natural habitat and ecosystem services in the Guangdong-Hong Kong-Macao “Megacity.” *Sustainability* 12(16):6675. <https://doi.org/10.3390/su12166675>
- Wang H, Liu Y, Zhang G, Wang Y, Zhao J (2021) Multi-scenario simulation of urban growth under integrated urban spatial planning: a case study of Wuhan, China. *Sustainability* 13(20):1–21. <https://doi.org/10.3390/su132011279>
- Waseem M, Halmy A, Gessler PE, Hicke JA, Salem BB (2017) Land use/land cover change detection and prediction in the north-western coastal desert of Egypt using Markov-CA. *Appl Geogr* 63:101–112. <https://doi.org/10.1016/j.apgeog.2015.06.015>
- Wubante FA, Boerema A, Nyssen J, Amare SM, Enyew AT, Passel SV (2020) Uncovering ecosystem services of expropriated land. *Land* 9(10):1–20. <https://www.mdpi.com/2073-445X/9/10/395/htm#>
- Yanping Q, Zhen W (2019) Study on urban expansion using the spatial and temporal dynamic changes in the impervious surface in Nanjing. *Sustainability* 11:933. <https://doi.org/10.3390/su11030933>
- Zhu Z, Zhou Y, Seto KC, Stokes EC, Deng C, Pickett ST, Taubenböck H (2019) Understanding an urbanizing planet: strategic directions for remote sensing. *Remote Sens Environ* 228:164–182. <https://doi.org/10.1016/j.rse.2019.04.020>
- Zhu J, Sun Y, Song S, Yang J, Ding H (2021) Cellular automata for simulating land-use change with a constrained irregular space representation: a case study in Nanjing city, China. *Environ Plan B: Urban Anal Nand City Sci* 48(7):1841–1859. <https://doi.org/10.1177/2399808320949889>